Does Economic Optimisation Explain LAI and Leaf Trait Distributions Across an Amazon Soil Moisture Gradient?

DR. SOPHIE FLACK-PRAIN (Orcid ID : 0000-0003-0711-5057)

Article type : Primary Research Articles

Does Economic Optimisation Explain LAI and Leaf Trait Distributions Across an Amazon Soil Moisture Gradient?

Running Title: Economic Optimisation of Canopy Dynamics

Sophie Flack-Prain[1], Patrick Meir[1,2], Yadvinder Malhi[4], Thomas Luke Smallman[1,3], Mathew Williams[1,3]

[1] School of GeoSciences, University of Edinburgh, Edinburgh, UK

[2] Research School of Biology, Australian National University, Canberra, ACT, Australia

[3] National Centre for Earth Observation, University of Edinburgh, UK

[4] Environmental Change Institute, School of Geography and the Environment, University of Oxford, Oxford, UK

Correspondence to: Sophie Flack-Prain (s.flack-prain@ed.ac.uk; +44 (0) 131 650 4757)

Supporting Information: Included

The authors state no conflict of interest

This article has been accepted for publication and undergone full peer review but has not been through the copyediting, typesetting, pagination and proofreading process, which may lead to differences between this version and the Version of Record. Please cite this article as doi: 10.1111/GCB.15368

Summary

Leaf-area-index (LAI) underpins terrestrial ecosystem functioning, yet our ability to predict LAI remains limited. Across Amazon forests, mean LAI, LAI seasonal dynamics, and leaf-traits vary with soil moisture-stress. We hypothesise that LAI variation can be predicted via an optimality-based approach, using net canopy C-export (NCE, photosynthesis minus the C-cost of leaf growth and maintenance) as a fitness proxy.

We applied a process-based terrestrial ecosystem model to seven plots across a moisture-stress gradient with detailed in-situ measurements, to determine nominal plant C-budgets. For each plot, we then compared observations and simulations of the nominal (i.e. observed) C-budget to simulations of alternative, experimental budgets. Experimental budgets were generated by forcing the model with synthetic LAI time-series (across a range of mean LAI and LAI seasonality) and different leaf-trait combinations (leaf mass per unit area, lifespan, photosynthetic capacity, and respiration rate) operating along the leaf-economic spectrum.

Observed mean LAI and LAI seasonality across the soil moisture-stress gradient maximised NCE, and were therefore consistent with optimality-based predictions. Yet, the predictive power of an optimality-based approach was limited due to the asymptotic response of simulated NCE to mean LAI and LAI seasonality. Leaf-traits fundamentally shaped the C-budget, determining simulated optimal LAI and total NCE. Long-lived leaves with lower maximum photosynthetic capacity maximised simulated NCE under aseasonal high mean LAI, with the reverse found for short-lived leaves and higher maximum photosynthetic capacity. The simulated leaf trait-LAI trade-offs were consistent with observed distributions.

We suggest that a range of LAI strategies could be equally economically viable at local-level, though we note several ecological limitations to this interpretation (e.g. between-plant competition). In addition, we show how leaf-trait trade-offs enable divergence in canopy strategies. Our results also allow an assessment of the usefulness of optimality-

based approaches in simulating primary tropical forest functioning, evaluated against in-situ data.

Keywords Optimisation, Canopy Dynamics, Leaf Traits, Tropical Rainforests, Fitness Proxy, Moisture-Stress

1. Introduction

Leaf area index (LAI, the total one-sided leaf area per unit ground area) determines canopy light interception, evapotranspiration and energy exchange between the land and atmosphere, driving significant spatial and temporal variability in carbon (C) assimilation (Caldararu *et al.*, 2012, Muraoka *et al.*, 2010, Street *et al.*, 2007, Xu & Baldocchi, 2004). Accordingly, LAI is a key property in the investigation of global biogeochemical cycles for both field and model-based studies (Baldocchi *et al.*, 1996, Carswell *et al.*, 2002, Sellers *et al.*, 1997). Principal determinants of global variation in LAI include moisture-stress, photoperiod, temperature and nutrients (Fisher *et al.*, 2012, Grier & Running, 1977, Iio *et al.*, 2014, Jolly *et al.*, 2005, Schleppi *et al.*, 2011, Wright *et al.*, 2013).

However, our ability to simulate spatial and temporal variation in LAI remains limited. Resolving this knowledge gap is important in the tropics (De Weirdt *et al.*, 2012, Kim *et al.*, 2012) as its forests, for instance those in the Amazon, have a large influence on the global C cycle (Liu *et al.*, 2017, Malhi *et al.*, 2008, Pan *et al.*, 2011) and climate system. Broad patterns across the Amazon basin are clear; mean LAI decreases and LAI seasonality increases with increasing soil moisture-stress, as forests shift from humid towards seasonally dry (Araujo-Murakami *et al.*, 2014, Malhi *et al.*, 2014). However, the climate sensitivity of phenological change remains unpredictable.

A key challenge in process-based modelling of LAI in tropical forests is to capture the phenological sensitivity to climatic forcings, via leaf senescence and leaf net primary productivity (NPP). Leaf-out timing and leaf turnover are often dependent on environmental factors including plant available water and radiation (Myneni *et al.*, 2007); however these processes are highly parameterised within models and lack a clear theoretical under-pinning (Table S1). Moreover, many models continue to simulate leaf NPP as a fixed fraction of total NPP (Clark *et al.*, 2011, Thornton & Zimmermann, 2007). Such model structures lack the capacity to actively vary LAI in

response to soil moisture-stress, particularly within the context of climatic change. As a result, current terrestrial biosphere and ecosystem models predict LAI dynamics poorly for Amazon forests across a range of dry season intensities: in a model-data comparison study for this region, Restrepo-Coupe *et al.* (2017) found that of the models tested (IBIS, ED2, JULES, and CLM3.5), only ED2 did not grossly overestimate mean LAI. Indeed, none of the models tested were able to capture dry season changes in LAI for equatorial forests. Xu *et al.* (2016) similarly found that while the ED2 model (with an updated PFT and hydrology scheme) was able to capture spatial patterns in LAI across the Central American region, it simulated mean LAI ca. $1 m^2 m^{-2}$ higher than MODIS estimates, and its simulated LAI seasonality was lower. However, it is important to note that uncertainty in MODIS LAI estimates is high in tropical regions (Liu *et al.*, 2018, Xu *et al.*, 2018).

The simulation of seasonal and annual LAI dynamics could be usefully improved via an optimality-based approach (Anten, 2016, Thomas & Williams, 2014). Such an approach assumes that plants aim to maximise fitness (i.e. optimise), where fitness is defined as the capacity to grow, reproduce and survive (Geber & Griffen, 2003, Violle *et al.*, 2007). Within an optimisation framework, leaf, root and stem growth, together with plant traits, are adjusted to maximise plant fitness. Net canopy C export (NCE; or variant of) is a commonly used fitness proxy (Franklin *et al.*, 2009, McMurtrie & Dewar, 2011, McMurtrie *et al.*, 2008). Akin to leaf level C optimisation approaches (Ackerly, 1999, Kikuzawa, 1991), NCE balances canopy level C gain via gross primary productivity (GPP) against C loss via growth (NPP_{Leaf}) and respiration (RM_{Leaf} and RG_{Leaf} ; leaf maintenance and leaf growth respiration respectively) (Givnish, 2002, Reich *et al.*, 2009).

$$NCE = GPP - NPP_{Leaf} - RM_{Leaf} - RG_{Leaf} \quad [1]$$

The maximisation of NCE is dependent on leaf traits, including but not limited to, photosynthetic capacity, leaf mass per unit area (LMA), leaf maintenance respiration rate, and leaf lifespan (Field, 1983, McMurtrie & Dewar, 2011). Leaf traits directly influence the rate of C gain via photosynthetic capacity. Leaf traits also directly influence C losses, including C used for leaf growth via LMA and leaf maintenance respiration via metabolic activity (Thomas *et al.*, 2019). In addition, leaf traits indirectly affect C assimilation and leaf maintenance C-costs, through the influence of leaf lifespan on total standing leaf biomass.

Leaf traits vary widely across the Amazon basin. Leaf nitrogen content is associated with photosynthetic capacity and maintenance respiration (Evans, 1989, Reich *et al.*, 2008), varying seven fold across Amazonia (6-41 mg g^{-1}) whilst LMA varies ten-fold (30-299 gm^{-2}) (Fyllas *et al.*, 2009) and individual leaf lifespans can range from less than two months to over four years (Reich *et al.*, 1991). Combinations of leaf traits have been shown to exist along a leaf-economic spectrum, exhibiting trade-offs among key trait-based axes of functionality (Wright *et al.*, 2005, Wright *et al.*, 2004, Wright & Westoby, 2002). 'Slow' leaf traits (i.e. long leaf lifespan, high LMA, low photosynthetic capacity and low metabolic rate) typically dominate in evergreen terra-firme forests (e.g. Carswell et al. 2000), whilst fast leaf traits (i.e. short leaf lifespan, low LMA, high photosynthetic capacity and high metabolic rate) are more prevalent in seasonally dry forests (Fyllas *et al.*, 2009, Givnish, 2002, Poorter & Bongers, 2006, Wright *et al.*, 2001). It is therefore critical to account for spatial variation in leaf traits, and their covariance, when investigating the interaction between NCE, LAI and soil moisture-stress across Amazon forests.

Optimality-based canopy models have had some success in predicting mean tropical LAI and its seasonality. For example, Caldararu *et al.* (2016) present a leaf phenology model which optimises net C assimilation (photosynthesis minus leaf maintenance C-costs) as a function of temperature, available light, soil water and leaf ageing. The model was able to explain 98% of spatial variation in tropical forest mean LAI, and 63% of variation in LAI amplitude (for the year 2006; where the model was parameterised on a pixel-by-pixel basis using a Markov Chain Monte Carlo fitting algorithm against MODIS LAI training-data for the years 2001-2005). However, Caldararu *et al.* (2016) did not compare fitted model parameters (which included photosynthetic efficiency, leaf maintenance C-costs, and leaf ageing rate) to ground-based estimates, nor did fitted parameters adhere to known inherent co-variation as a result of physiological trade-offs (Osnas et al., 2013). Elsewhere, leaf lifespan has been presented as an emergent property of carbon optimality modelling, evaluated against observation data (Xu *et al.*, 2017). While optimality-based canopy models have been applied globally, model evaluation against tropical forests field estimates of C fluxes (i.e. GPP, NPP and respiration) has been limited (Caldararu *et al.*, 2014, Vico *et al.*, 2017). Furthermore, current approaches have yet to explore how observed variation in traits (photosynthetic capacity, LMA, leaf maintenance respiration rate, and leaf lifespan) affect C-cost and gain dynamics. Until now, a lack of fundamental information on C uptake, allocation,

metabolism and plant traits has limited the scope for more detailed optimisation theory testing against tropical forest in-situ data.

To this end, we use the process-orientated terrestrial ecosystem Soil-Plant-Atmosphere model (SPA), to investigate LAI optimality through analysis of plant C and water cycles, for forest plots with detailed C budget measurements across an Amazonian moisture-stress gradient. Previous work calibrating SPA to plots across the moisture-stress gradient, has shown that modelled C dynamics are consistent with field estimates (Flack-Prain *et al.*, 2019), and therefore provide a basis for model experimentation of C dynamics.

Our key science questions are:

1. How does (a) mean LAI and (b) LAI seasonality impact NCE trade-offs between leaf C costs and C assimilation across the moisture-stress gradient
2. Are in-situ LAI measurements consistent with optimality-based predictions?
3. How do trait trade-offs across the leaf economic spectrum impact optimal LAI dynamics?

For question one, we hypothesise that leaf growth and maintenance C-costs increase with mean LAI independent of climate (Figure 1). In the absence of drought, GPP increases with mean LAI (prior to shading effects), making high LAI an optimal strategy. Under high moisture-stress, GPP is increasingly limited at higher LAI, resulting in a lower optimal leaf area. With respect to LAI seasonality (see Equation 2), we hypothesise that under low seasonal moisture-stress leaf C-costs increase with LAI seasonality. High LMA and faster leaf turnover result in higher leaf growth costs. In addition, (annual) GPP decreases as LAI seasonality increases. As a result, we predict aseasonal LAI will be optimal for forests with more consistent year-round rainfall. Conversely, where seasonal moisture-stress is high, we predict leaf C-costs decline as LAI seasonality increases. Maintenance respiration costs decrease alongside seasonal declines in LAI. GPP does not increase as LAI seasonality declines if GPP is limited by seasonal moisture-stress. We therefore hypothesise that higher LAI seasonality will be economically optimal in sites with stronger seasonal climates. As such we predict that in response to question two, C cycle dynamics under optimal mean LAI and LAI seasonality (i.e. that which maximises NCE) will reflect and explain in-situ data.

For question three we investigate how NCE responds to changes in leaf traits (photosynthetic capacity, LMA, leaf maintenance respiration rate, and leaf lifespan). Leaf traits determine C-costs

of canopy construction and longevity, which influence the economics of optimisation. Therefore, an alternative hypothesis is that variation in leaf traits will allow aseasonal LAI even in seasonal climates. Optimal leaf traits (i.e. that which maximise NCE) are predicted to match observed trait distributions across the moisture-stress gradient. Furthermore, we hypothesise that leaf traits and LAI will be inextricably linked, and that optimal leaf trait strategies will depend on LAI and vice versa.

Optimisation approaches could offer a unique opportunity to reduce uncertainty in predictions of Amazon phenology, and consequently C fluxes. This study will test the suitability of a C economic optimisation approach to predict ecosystem functioning in response to soil water limitation. We use Amazon permanent sample plots with uniquely detailed time-series measurements of C fluxes and LAI, together with a comprehensive suite of leaf trait estimates (Doughty *et al.*, 2015, Fyllas *et al.*, 2009, Malhi *et al.*, 2015). We simulate a range of mean LAI and LAI seasonalities and evaluate their optimality by comparing their NCE. This approach allows us to present comprehensive predictions about the sensitivity of NCE to LAI. Furthermore, we are able to present trade-offs in C allocation dynamics, leaf traits, and soil moisture-stress, referenced against in-situ data. We discuss the potential for optimisation approaches to improve earth system model predictions of canopy properties and C cycling.

2. Materials and Methods

2.1 Site Characteristics

This study uses field data from Amazon forests sites of the Global Ecosystem Monitoring network (GEM; Malhi et al., 2015). We focus on seven one-hectare permanent sample plots along moisture-stress gradients in the east and west Amazon, distributed across four locations (Table 1). Moisture-stress across plots is quantified using maximum climatological water deficit (MCWD), a measure of seasonal water deficit where more negative values relate to larger water deficit, and potentially greater moisture-stress (the focal MCWD gradient spans -86 to -498 mm; see supporting information, SI, for MCWD equation). Soil and species composition differs between localised plots, with little evidence of anthropogenic disturbance (Malhi *et al.*, 2015). A short description of each plot is given here, with further details on site characteristics available in Aragao *et al.* (2009), Quesada *et al.* (2012), Metcalfe *et al.* (2010), Araujo-Murakami *et al.* (2014), Malhi *et al.* (2014), Doughty *et al.* (2015), Malhi *et al.* (2015) and Rocha *et al.* (2014).

Core terra-firme Amazon forest plots, CAX04 and CAX06 are located in the Caxiuanã National Forest in Para State, Brazil and occupy the least moisture-stressed zone of the gradient (MCWD -86mm). TAM05 and TAM06, located in the Tambopata Biological Reserve in the Madre de Dios region of Peru, are subject to a moderate dry season (MCWD -256mm). Transitional forest plots - KEN01 and KEN02 - are situated in the Hacienda Kenia in Guarayos Province, Santa Cruz, Bolivia, and are subject to a more intense dry season (MCWD -342mm). The Tanguro plot, located in the Fazenda Tanguro, Mato Grosso State, Brazil, occupies the highest moisture-stress zone along the gradient (MCWD -498mm).

2.2 LAI and Leaf Trait Dynamics across the Soil-Moisture Gradient

We used linear regression models to provide an overview of the spatial covariation of observed annual mean LAI, LAI seasonality and leaf traits across the MCWD gradient (see supporting information, SI, for full details on LAI and leaf trait measurements). In the analysis we also included precipitation seasonality (%) as a characteristic of precipitation regime (see section 2.5 for calculation).

2.3 The Soil-Plant-Atmosphere Model

SPA is a process-based hydrodynamic, terrestrial ecosystem model (Williams *et al.*, 1996), which has previously been calibrated and evaluated against measured C and water fluxes for moist tropical forests in Caxiuanã (eastern Amazon) and Manaus (central Amazon) (Fisher *et al.*, 2007, Williams *et al.*, 1998). The pathways through which soil moisture LAI, and leaf traits impact C assimilation and leaf C costs (i.e. NCE) in SPA are summarised in Figure 2, and are described below.

SPA simulates the vertical distribution of canopy layer specific energy-balance, heat and mass exchange, including photosynthesis and transpiration for up to 10 canopy layers (Bonan *et al.*, 2014, Williams *et al.*, 1996). Each canopy layer in SPA is further partitioned between sunlit and shaded fractions. The radiative transfer scheme determines the canopy interception of radiation (following Beer-Lambert's Law) and its subsequent transmittance, reflectance and absorption of long wave, near infra-red and direct and diffuse photosynthetically active radiation (PAR) for each canopy layer and the soil surface (Williams *et al.*, 1998). The long wave radiation balance is updated by the impact of the soil and canopy energy balance on temperature (Smallman *et al.*, 2013). Boundary layer exchange is subject to the decay of wind speed above and within the canopy profile modified by the impact of the surface energy balance on turbulent exchange

(Smallman *et al.*, 2013). The vertical distribution of nitrogen (N) within the canopy is represented as an exponential decay function (Williams *et al.*, 1996). At the leaf level, the Farquhar model is used to determine photosynthesis (Farquhar & Von Caemmerer, 1982). The Penman-Monteith equation is used to estimate transpiration.

SPA simulates leaf-level C and water fluxes through eco-physiological principles governing stomatal opening, balancing atmospheric demand for water and available supply from the soil to optimise photosynthesis (Bonan *et al.*, 2014, Smallman *et al.*, 2013, Williams *et al.*, 2001, Williams *et al.*, 1996). The stomatal conductance model in SPA optimises leaf C gain per unit nitrogen within the limits of water supply, therefore preventing leaf water potential dropping below a critical value. The model thereby combines an intrinsic water use efficiency and hydraulic safety, to optimise simulated stomatal conductance (Bonan *et al.*, 2014, Fisher *et al.*, 2006). The rate of liquid phase supply is dependent on plant water storage, soil water potential, and soil-to-leaf hydraulic resistance (Williams et al., 1996; William et al., 2001). In SPA, sap flow is buffered by stored plant water. Simulated soil water inputs via precipitation account for canopy interception, and subsequent evaporation and drainage. Soil water retention curves then relate soil texture to water transfer through the soil profile (Saxton *et al*., 1986). Soil water content and soil radiation balance is used to calculate water evaporation from the soil surface (Amthor *et al.*, 1994). Root water uptake is computed as a function of root dimensions (surface area, biomass and depth) and soil hydraulic conductivity. Root resistivity and root biomass per unit soil volume determine root-to-stem conductance (Williams *et al.*, 2001). Aboveground hydraulic conductance is calculated assuming resistance to xylem water supply increases with the height of the canopy layer (Williams *et al.*, 1996). As in a pipe model, each canopy layer has an independent water supply system.

Phenology in this application of SPA was forced using LAI timeseries (Figure 2). Foliar C stocks at a given timestep were computed as a function of LAI and leaf C per unit area (see SI for equations). Leaf NPP was calculated as the difference between the foliar C stock of the current timestep and that of the previous timestep following leaf litterfall. Leaf NPP was determined prior to other plant NPP components. Where the leaf NPP requirement exceeded total NPP for the given timestep, the non-structural C (NSC) pool was drawn upon. When the NSC pool became depleted, a fraction of NPP was redirected towards NSC storage in subsequent timesteps when leaf NPP did not exceed total NPP. Leaf litterfall in SPA was simulated as a function of day of peak leaf fall,

leaf fall period and potential leaf lifespan (see SI for equations). The parameters were calibrated against plot litterfall data. Where leaf litterfall was insufficient to support a decline in forced LAI across two timesteps, the deficit was added to the leaf litterfall pool. When not forced with in-situ LAI, the capacity of SPA to simulate canopy dynamics has been demonstrated by both López-Blanco *et al*. (2018) and Sus *et al*. (2010).

Root and wood C allocation and turnover is simulated by the sub model DALEC2 (Bloom & Williams, 2015). Following the subtraction of foliar NPP from the total NPP pool, the remaining NPP was distributed between roots and wood as a function of fixed, plot-specific allocation fractions. Root and wood turnover was simulated as a function of component C stock using a fixed, plot-specific turnover rate parameter.

Autotrophic respiration in SPA was computed on a mass basis. Leaf respiration was calculated as a function of leaf N content (Flack-Prain *et al.*, 2019, Reich *et al.*, 2008) and total leaf C stock (see SI). Wood and fine root maintenance respiration were estimated as a function of component C stock and a respiration coefficient parameter. When calculating wood respiration there was no distinction between sapwood and heartwood. Growth respiration was calculated as a fixed proportion of NPP (0.28) (Waring & Schlesinger, 1985). Within SPA, C allocation to respiration was executed before allocation to growth.

2.4 Model Set-up, Calibration, and Evaluation

We used field estimates of plant traits, initial C stocks, soil texture, meteorology and LAI to drive SPA (Figure 2) at each permanent sample plot across the GEM network (see SI). Specifically, the model was parameterised using local estimates of: soil texture, soil C stock, leaf N content, LMA, photosynthetic capacity ($\kappa_{c,}$ and κ_J ; V_{cmax} and J_{max} normalised by leaf N content respectively), the fraction of NPP allocated to fine roots and wood, root depth, foliar, wood and fine root C stocks, and wood and fine root respiration coefficients. Fine root and wood turnover rates were assumed proportional to component NPP (given the maturity of stands and their disturbance history). Wood and root respiration measurements were used together with component C stocks to estimate plot-specific wood and root respiration coefficients. SPA hydraulic conductance parameters derived from detailed field measurements at an Amazon moist forest site were used in model runs for all plots (Fisher *et al.*, 2007, Fisher *et al.*, 2006, Rowland *et al.*, 2015a). Hydraulic conductance parameters include stem conductance, minimum leaf water potential, intrinsic water use efficiency, leaf capacitance, and root resistivity. Hourly meteorological forcing data were supplied

from weather stations located within 1km of the study plots. Data gaps in air temperature, wind speed, shortwave radiation and vapour pressure deficit records which were less than six consecutive hours were estimated by spline interpolation. Data gaps greater than six hours, or gaps in precipitation measurements were filled using hourly spline-interpolated and bias corrected ERA-Interim data (Dee *et al.*, 2011). Solar zenith angle was accounted for when interpolating solar radiation values. Monthly LAI measurements were scaled to daily estimates via linear interpolation to force simulated LAI.

Time-series field measurements of soil moisture and leaf litterfall were used to calibrate simulated soil water drainage parameters and leaf fall parameters respectively. Within SPA, the empirical model used to simulate soil hydraulics (Saxton et al., 1986, eqn. 10) was calibrated by adjusting the slope of the interaction between soil texture and water retention, to reflect tropical soil moisture dynamics (to within standard error estimates of annual mean soil moisture). Modelled leaf litterfall was calibrated to accurately simulate litterfall period and amplitude (within standard error estimates of annual litterfall), using field measurements to retrieve model parameters on leaf fall timing, duration and potential leaf lifespan (Table 2).

SPA was evaluated against independent field estimates of annual ecosystem C fluxes, including NPP, GPP, NCE and autotrophic respiration. Total NPP and autotrophic respiration were calculated as the sum of measured leaf, root, and wood NPP and respiration respectively. GPP was calculated as the sum of total measured NPP and autotrophic respiration, and NCE was calculated as the sum of measured root and wood NPP and respiration (i.e. GPP minus leaf NPP and respiration).

The calculation of model uncertainty as a result of parameter error was limited to that associated with LAI estimates, as the availability of uncertainty estimates for leaf traits and rooting properties was plot-dependent, and there were no uncertainty estimates for hourly meteorological data or soil properties. Model uncertainty estimates were calculated by simulating C fluxes for each plot under the upper and lower standard error of monthly LAI field measurements. Following model calibration, simulated C fluxes were evaluated against field estimates of GPP, respiration and NPP, using linear regression models. Field estimates were derived from a suite of biometric time-series measurements including dendrometers, root ingrowth cores, infra-red gas analysers and litterfall traps (Doughty *et al.*, 2015), further details of which can be found in the SI.

2.5 Modelling C Cycle Sensitivity to LAI and Soil Moisture-Stress Interactions

We tested whether the maximisation of NCE explained observed mean LAI and LAI seasonality across the MCWD gradient. We forced the model at each plot using a suite of synthetic LAI time-series, and retrieved the resultant C budget. For each plot, during model experiments; meteorology, soil texture, the fraction of NPP allocated to wood and roots (following leaf NPP allocation), initial C stocks and leaf traits were kept constant. To generate the synthetic LAI time-series, we systematically varied mean LAI (Figure S2) and LAI seasonality (Figure S3) against the observation data at each plot. First, to vary mean LAI, for each plot, we adjusted the annual mean to between 1-8 m^2 m^{-2} at 0.5 m^2m^{-2} intervals, conserving the nominal seasonal cycle (n=105; 7 plots × 15 synthetic LAI time-series). Second, we constructed synthetic LAI time-series for each plot (n= 63; 7 plots × 9 synthetic LAI time-series), which conserved nominal mean LAI, but varied LAI seasonality (Table S2).

The timing of LAI_{min} in the synthetic LAI time-series were aligned with seasonal lows in the observation dataset. LAI seasonality (LAI_s; %), was calculated as the average difference between monthly LAI and the annual mean:

$$LAI_s = \frac{\sum_{i=1}^{n} \frac{|LAI_i - \overline{LAI}|}{\overline{LAI}} \cdot 100}{n} \quad [2]$$

Where LAI_i is LAI for a given month, $\overline{LAI}$ is nominal mean LAI, and n is the number of months in the time-series. Estimates of local precipitation seasonality (used in regression analyses to relate LAI and leaf trait distributions to precipitation regime) were calculated using an analogous equation, where LAI_i was substituted for precipitation in a given month, and $\overline{LAI}$ was substituted for mean monthly precipitation.

For each LAI timeseries (observed or synthetic), model simulations were run using local climate data, allowing sufficient iterations for C cycle feedbacks on component C pools to reach steady state (300 years). We computed the interaction between C assimilation, the C-cost of leaf growth and maintenance (i.e. GPP and NCE), and mean LAI/LAI seasonality for each plot. We compared nominal annual mean LAI to that under the simulated maximum NCE. We then compared field estimated and model simulated NCE under nominal LAI, to the maximum simulated NCE retrieved from synthetic LAI time-series runs (for mean LAI and LAI seasonality). Field estimated error was the propagated standard error of components (i.e. GPP, leaf NPP, and leaf respiration).

Optimal mean LAI and LAI seasonality was defined as that which maximised NCE under the plot conditions.

2.6 Leaf Trait Interactions with NCE along Soil Moisture Gradients

We tested the impact of leaf traits on optimal LAI across the MCWD gradient. We focused on exploring the extremes of the moisture gradient, choosing plots with typically drier (KEN02) and moister (CAX04) climate and soils to simplify the analysis. We used the fast leaf traits observed at the drier KEN02 plot (i.e. short leaf lifespan, low LMA, high photosynthetic capacity and high metabolic rate), and the slow leaf traits nominal at the moister CAX04 plot (i.e. long leaf lifespan, high LMA, low photosynthetic capacity and low metabolic rate; Table 2), to construct model forcings for a fast and slow leaf trait cohort. At both plots, we forced the model with the fast and slow leaf trait cohort, under the suite of synthetic LAI time-series outlined in the previous section (n=100; for mean LAI 2 plots × 15 synthetic LAI time-series × 2 leaf trait strategies, plus for LAI seasonality, 2 plots × 10 synthetic LAI time-series × 2 leaf trait strategies) and retrieved simulated NCE. As before, for each plot we kept meteorology, soil texture, the fraction of NPP allocated to wood and roots, and initial C stocks constant. We compared the interaction between NCE and mean LAI/LAI seasonality, under the different leaf trait cohorts, on drier and moister soils. We then contrasted field estimated and model simulated NCE under nominal LAI-leaf trait distributions, to the maximum simulated NCE retrieved from synthetic LAI-leaf trait runs.

3. Results

3.1 Model Calibration and Evaluation

SPA was calibrated to effectively simulate soil moisture and leaf litterfall variation and dynamics across sites (Table 3, Figures 3 & S5). SPA-simulated GPP was within field estimate error bounds for five of the seven plots (Figure S5; the disparity between error bounds for the remaining two plots was marginal at 115 gC m^{-2} yr^{-1} and 50 gC m^{-2} yr^{-1} for KEN01 and TAM06 respectively). The GPP-MCWD interaction was consistent between simulated GPP and estimates derived from field measurements (slope of GPP~MCWD interaction; SPA=2.4±0.8; GEM =2.0±0.9). Modelled and observed NCE were significantly correlated across plots (R^2=0.62, p=0.04). A breakdown of model performance with respect to leaf, root, and wood NPP and respiration, is described in Flack-Prain *et al.* (2019). Model calibration and evaluation results are presented in full in the SI.

3.2 LAI and Leaf Traits Trends along the MCWD Gradient

Canopy and leaf level properties co-varied across the MCWD gradient (Figure S6; Table 4). Mean annual LAI decreased as precipitation seasonality increased (R^2=0.57, p=0.05). LAI seasonality increased in line with precipitation seasonality (R^2=0.87, p=0.002). Congruously, a significant negative interaction existed between mean annual LAI and LAI seasonality (R^2=0.79, p=0.008). Across the canopy-to-leaf scale, mean annual LAI increased significantly with LMA (R^2=0.86, p=0.002). Mass based foliar N content decreased significantly with mean annual LAI, and increased significantly with LAI seasonality (R^2=0.92, p<0.001 and R^2=0.77, p=0.009 respectively). At the leaf-level, a significant negative correlation existed between LMA and mass based foliar N content (R^2=0.85, p=0.003). Correspondingly, mass based foliar N exhibited a significant negative correlation with calibrated leaf lifespan (R^2=0.57, p=0.05).

3.3 Impact of Mean LAI on NCE Trade-Offs across the Soil-Moisture Gradient

As a result of leaf C cost and C assimilation trade-offs, high mean LAI was economically deleterious within the model experiment for forest plots occupying drier soils, but remunerative for those occupying moister soils (Figure 4). Simulated leaf C-costs (via growth and maintenance) increased linearly with mean LAI. In contrast, simulated GPP increased with mean LAI for five of the seven plots. The rate of GPP increase slowed as mean LAI increased (Figure 4). At Tanguro and KEN02 (which occupy drier soils), GPP did not increase with mean LAI beyond an upper limit (5.5 – 6.0 m^2m^{-2}); at higher LAI GPP declined towards zero. The modelled decline of GPP to zero was due to reduced C availability for non-foliar growth (at high mean LAI) leading to an eventual collapse in fine root biomass stocks, whereby canopy function was no longer supported. The simulated response of leaf C-costs and C assimilation to mean LAI caused NCE to be progressively reduced at high mean LAI as soil moisture-stress strengthened. Consequently, simulated optimal mean LAI (i.e. LAI at which NCE was maximised; LAI_{Opt}) declined as moisture-stress increased (Figure 5a; mean LAI_{Opt}~ MCWD R^2=0.72, p=0.02).

3.4 Consistency between In-Situ LAI Measurements and Optimality-Based Predictions from Mean LAI Experiment.

In-situ measured LAI (LAI_{field}) maximised NCE without matching predicted optimal mean LAI (Figure 5a). Field measurements of NCE correlated significantly with simulated optimal NCE (NCE_{Opt}; Figure 6; R^2=0.83, p=0.004). Modelled NCE when SPA was forced with observed LAI was also consistent with NCE_{Opt} (R^2=0.94, p<0.001). Yet, LAI_{field} did not correlate significantly

with simulated mean LAI_{Opt} (mean LAI_{Opt}~ LAI_{field} R^2=0.29, p=0.21). Across the moisture-stress gradient, predicted mean LAI_{Opt} was 22.6% higher than LAI_{field}. Simulated mean LAI_{Opt} was within field observation error at three out of seven plots. In-situ measurements of LAI were simultaneously consistent with optimality-based predictions (i.e. maximised NCE), but inconsistent with predicted optimal LAI, because of the asymptotic response of simulated NCE to mean LAI over 1-2 m^2m^{-2} differences in leaf cover (Figure 4).

3.5 Impact of LAI Seasonality on NCE Trade-Offs across the Soil-Moisture Gradient

Trade-offs between leaf C costs and C assimilation resulted in seasonal LAI being deleterious within model simulations for forests occupying moister soils (Figure 6). However, for forests occupying drier soils, a wide range of LAI seasonalities proved equally optimal. For forest plots occupying moister soils, simulated GPP declined with increasing LAI seasonality (Figure 7). For forest plots occupying drier soils, simulated GPP reached an asymptote across LAI seasonalities of between 0-40%, declining thereafter. Across all plots, the modelled C-cost of leaf growth and maintenance increased with LAI seasonality. However, the slope of the leaf C cost-LAI seasonality interaction was reduced for drier plots. At low moisture-stress, the response of leaf C costs and C assimilation to LAI seasonality caused simulated NCE to decline with increasing LAI seasonality. At high moisture-stress simulated NCE varied little across a range of LAI seasonalities before declining. As a result, simulated optimal LAI seasonality increased significantly with moisture-stress (LAI_{Opt} seasonality ~ MCWD R^2=0.61, p=0.04; Figure 5b).

3.6 Consistency between In-Situ LAI Measurements and Optimality-Based Predictions from LAI Seasonality Experiment.

Akin to trends in mean LAI, field measured LAI seasonality maximised NCE, but did not match the predicted optimal LAI seasonality. Across the moisture-stress gradient, NCE_{field} correlated significantly with predicted NCE_{Opt} (NCE_{Opt} ~ NCE_{field} R^2=0.60, p=0.04, RMSE= 257.5 gC m^{-2} yr^{-1}, bias=6.5%). Modelled NCE when SPA was forced with observed LAI was also consistent with predicted NCE_{Opt} (NCE_{Opt} ~ NCE_{SPA} R^2=0.98, p<0.001, RMSE=43.1 gC m^{-2} yr^{-1}, bias=1.2%). LAI_{field} seasonality did not correlate significantly with simulated LAI_{Opt} seasonality (LAI_{Opt} seasonality ~ LAI_{field} seasonality R^2=0.08, p=0.5). As before, field measured LAI seasonality supported optimal NCE without matching the simulated optimal LAI seasonality, because of the asymptotic response of simulated NCE across a range of LAI seasonalities (Figure 7).

3.7 Leaf Traits Interactions with the NCE along the Soil Moisture Gradient

Slow leaf traits were optimal (i.e. maximised simulated NCE) under high mean LAI, whilst fast leaf traits were optimal under low mean LAI (Figure 8). Simulated LAI_{Opt} was 2.5 m^2 m^{-2} higher under slow leaf traits compared to fast leaf traits, independent of moisture-stress (Figure 8 upper panels). Under high moisture-stress, slow leaf traits outperformed fast leaf traits (with respect to simulated NCE maximisation) for LAI > $4m^2m^{-2}$. The transition point increased to ~5.5 m^2 m^{-2} under low moisture-stress. When the model was forced with local, observed LAI at the low moisture-stress plot, there was no significant difference in simulated NCE between nominal-slow and alternate fast leaf traits (nominal-slow 2709±301 gC m^{-2} yr^{-1}; alternate fast 2846±73 gC m^{-2} yr^{-1}). Under high moisture-stress, when the model was forced with observed LAI, NCE was 33% higher for nominal-fast traits compared to alternate slow leaf traits (nominal-fast 1647±41 gC m^{-2} yr^{-1}; alternate slow 1238±57 gC m^{-2} yr^{-1}). The interaction between optimal leaf trait strategy and mean LAI matched the observed coordination between leaf and canopy properties across the moisture-stress gradient.

Under high moisture-stress, fast leaf traits were optimal across a range of LAI seasonalities (Figure 8). Under low moisture-stress, aseasonal LAI was optimal regardless of leaf trait strategy. At the drier forest plot, fast leaf traits generated stable simulated NCE across LAI seasonalities of 0-25%, declining thereafter. At the moister forest plot, simulated NCE was maximised under aseasonal LAI; at 0% LAI seasonality under fast leaf traits; and at 0.17% LAI seasonality under slow leaf traits. Under high moisture-stress, simulated LAI_{Opt} seasonality was 22% under fast leaf traits, which is close to LAI_{field} seasonality at 18%. Similarly, under low moisture-stress, simulated LAI_{Opt} seasonality was 0.17% under slow leaf traits which matches observed LAI_{field} seasonality at 0.2%.

4. Discussion

Our aim was to test if key ecosystem properties (i.e. LAI dynamics and leaf trait suites) along a tropical forest MCWD gradient could be predicted using an optimality-based approach. We computed the sensitivity of NCE (representing C economic trade-offs, i.e. C assimilation minus leaf growth and maintenance C-costs) to moisture-stress across a spectrum of LAI strategies using a detailed process based model of C uptake, allocation and turnover. As moisture-stress increases, optimal mean LAI (i.e. that which maximised NCE) decreases, and optimal LAI seasonality increases. However, an asymptotic response of NCE to mean LAI and LAI seasonality limits the

predictive power of an optimality-based approach (Figure 4); optimal LAI estimates do not match in-situ observations closely. We went further, to evaluate the sensitivity of C cycle dynamics to coincident variation in leaf traits, LAI and moisture-stress. For forest plots occupying moister soils, slow leaf traits (i.e. long leaf lifespan, high LMA, low photosynthetic capacity and low metabolic rate) are optimal under aseasonal, high LAI. For forest plots occupying drier soils, fast leaf traits (i.e. short leaf lifespan, low LMA, high photosynthetic capacity and high metabolic rate) are optimal under low LAI (across LAI seasonalities of 0-20%). Predicted optimal combinations of mean LAI, LAI seasonality and leaf traits reflect observed dynamics across the moisture-stress gradient.

4.1 Divergence in Canopy Economics across the MCWD Gradient Drives Optimal LAI

Model experiments indicated that at the drier end of the moisture gradient high LAI canopies are economically unfavourable (Figure 4). Any C gains (via photosynthesis) from additional leaf area are outweighed by the increase in leaf growth and maintenance C-costs. Thus, consistent with our hypothesis, simulated NCE was maximised in drier forests by seasonal, low mean LAI (Figures 4 & 5). Under moister conditions, simulated NCE was maximised by aseasonal, high mean LAI. Photosynthetic gains are maintained with high LAI canopies, and are economical, as soil moisture is a less limiting factor.

4.2 Maximisation of NCE does not Predict In-Situ LAI

As hypothesised, in-situ LAI measurements maximise NCE and are therefore consistent with optimality-based predictions (Figure 6). Yet, simulated optimal LAI is a relatively poor predictor of observed LAI dynamics (Figure 5). Simulated NCE responds asymptotically to changes in LAI seasonality at drier plots (Figure 7), and mean LAI (Figure 4). For example, NCE can vary little across a mean LAI range of ca. $2 m^2 m^{-2}$ and a LAI seasonality range of up to 40% because of the complex trade-offs in the C economy linked to structural-functional interactions. This low sensitivity allows a range of mean LAI/LAI seasonalities to be similarly economically viable. As a result, despite matching optimality-based predictions (i.e. maximising NCE), mean LAI_{field} is not itself predicted well purely by the maximisation of NCE. Additional constraints to LAI_{field} beyond C-economics are then under-determined.

Nutrient limitation was not accounted for in this analysis, but could be the additional constraint needed to improve optimality-based LAI predictions. Where moisture-stress is low, but nutrients are limited (i.e. Caxiuanã) optimal LAI exceeds in-situ measurements (Figure 4). Kumagai *et al.*

(2006) report higher LAIs of up to 6.8 m^2m^{-2} ($\bar{x}$ = 6.2 m^2m^{-2}) in Bornean forests. Limited measurements indicate that soil nitrogen and pH across the Lambir Hills region are higher than at the Caxiuanã plots, as is soil phosphorus (CAX04 only) (Davies *et al.*, 2005, Malhi *et al.*, 2015, Quesada *et al.*, 2010). Furthermore, field evidence shows that total leaf litterfall is positively associated with soil richness (Chave *et al.*, 2010), and thus soil nutrient availability is likely to have a determinate effect on LAI dynamics. We suggest that foliar N and P demands may preclude otherwise optimal, higher LAI, in nutrient poor forests.

Alternatively, the disparity between predicted optimal-LAI and in-situ LAI measurements could be a result of a focus solely on foliar investment. One hypothesis is that returns on canopy investment could decline relative to returns from investing in other tissues which support leaf function; for example, investment in roots for nutrient acquisition (e.g. Thomas and Williams (2014)). The inclusion of investment returns across plant components could potentially reduce the range of equally viable LAI dynamics under current model assumptions. Haverd *et al.* (2016) have demonstrated optimisation of above versus belowground allocation to capture canopy dynamics across an Australian precipitation gradient. Another hypothesis is that LAI optimisation is sensitive to a reduction in marginal return rate (i.e. as the relative increase in net C gain starts to decline, plants may cease allocation towards the canopy). Further investigation into the presented model simulations show that if a marginal return rate function is added, whereby LAI ceases to increase when NCE is within <100 gC m^{-2} yr^{-1} of the maximum, mean LAI is more successfully predicted (R^2=0.56, p=0.05, compared to simulated mean LAI_{Opt} ~ LAI_{field} R^2=0.29, p=0.21).

Differences between simulated optimal LAI and observed LAI could also result from the radiative transfer scheme used. Braghiere *et al.* (2019) recently found that the inclusion of leaf clumping into the radiative transfer scheme alleviated light limitation in lower canopy layers, especially where LAI was high (i.e. in the tropics). GPP increased as a result. However, leaf clumping was not simulated within SPA as local clumping estimates are unavailable for this study. Further work could therefore usefully test the sensitivity of NCE and LAI optimality to radiative transfer schemes.

With respect to LAI seasonality, the viability of both seasonal and aseasonal LAI at drier forest plots is ecologically consistent with the expectation that high climatic seasonality promotes the coexistence of different LAI strategies (i.e. deciduous-evergreen) (Sakschewski *et al.*, 2015). Furthermore, it is also consistent with in-situ observations. For example, at the Kenia plots, both

deciduous (e.g. *Hura Crepitans* L.) and evergreen (e.g. *Dendropanax arboreus*) species are present (Abelho *et al.*, 2005, Figueroa-Esquivel *et al.*, 2009, Poorter & Bongers, 2006). Given the interaction between LAI seasonality and leaf trait strategy, we might expect community trait composition to also support a range of viable strategies (see section 4.5).

4.3 Should Optimisation of Whole Stand C Dynamics Predict In-situ LAI?

In addition to asking why optimisation of whole-stand NCE does not predict observed LAI, we ask whether indeed it should (Anten & During, 2011). To date, optimality-based ecosystem models and DGVMs have had varied success in predicting mean and seasonal LAI values that are consistent with field observations (De Kauwe *et al.*, 2014, McMurtrie *et al.*, 2008, Thomas & Williams, 2014, Walker *et al.*, 2014b), and efforts have typically focused on single, mono-specific stands. In a mixed-species forest where a variety of plant strategies co-exist, LAI which exceeds the forest-wide optimum would increase competitiveness in individual trees (Anten, 2016). van Loon *et al.* (2014) demonstrated how the inclusion of stem competition improved optimality-based predictions of LAI. However, given that in our study LAI_{field} was typically lower than simulated optimal LAI, including competition would not reduce the disparity between our optimality-based predictions and in-situ LAI measurements. Furthermore, the disparity between observed and simulated optimal LAI could be the result of our fitness proxy selection (Dewar *et al.*, 2009). Whilst NCE has proved a suitable measure of plant fitness elsewhere (McMurtrie & Dewar, 2011), it does not capture all aspects of plant fitness. It is possible that the appropriateness of NCE as a fitness proxy shifts as drought, nutrient limitation and disturbance increase, and plants must balance investment risk against shorter-term C gains.

4.4 Leaf Traits Determine Optimal LAI

Simulated optimal mean LAI is dependent on leaf traits. Within model experiments, independent of precipitation regime, fast leaf traits support low mean LAI, while slow leaf traits support high mean LAI (consistent with in-situ data) (Figure 8; Table 2). As LAI increases, photosynthesis per unit leaf area declines. Consequently, under fast leaf traits high respiratory C-costs begin to outweigh C gains from high photosynthetic capacity. Conversely, lower respiratory C-costs under slow leaf traits are sustainable as leaf area increases.

We show that leaf traits do not influence simulated optimal LAI seasonality at the moister forest plot where aseasonal LAI is most remunerative (Figure 8). However, at the drier forest plot, slow leaf traits are most remunerative under aseasonal LAI only, while fast leaf traits support a wider

range of LAI seasonalities (0-20%). Low leaf growth C-costs and high photosynthetic capacity allow fast leaf traits to support different LAI seasonalities (though notably at low mean LAI). Slow leaf traits were unable to achieve the same viable range in LAI seasonality, as the increase in new leaf growth (following seasonal turnover) had a higher C-cost (due to high LMA).

4.5 Fast and Slow Leaf Traits Both Maximise Fitness in Dry Forest Plots, but at Different LAI

Model experiments, at drier forest plots, showed that fast and slow leaf trait strategies are equally viable, but at different mean LAI (Figure 8). These findings align with early conceptual approaches which used cost-benefit analyses to demonstrate how links between leaf longevity and phenology in temperate forests support coexistence of evergreen and deciduous trees (Kikuzawa, 1991, Kikuzawa, 1996). Reporting on dry tropical evergreen and deciduous forests in Cambodia, Ito *et al.* (2007) focused on sites located within 15 km which were thus assumed to be under the same precipitation regime. The evergreen forest had a mean LAI of 4.05 m^2m^{-2}, while the deciduous forest had a much lower mean LAI of 0.88 m^2m^{-2}. The difference in LAI is similar to that reported in this study, between predicted optimal LAI under slow and fast leaf traits at the dry forest plot (~2.5 m^2m^{-2}). Our results are also consistent with that of Sakschewski *et al.* (2015), who predict that variability in plant strategies should be highest in drier, seasonal areas. Our findings suggest that trait trade-offs across the leaf economic spectrum offer alternative routes to viable strategies, supporting different forest types under similar climates.

4.6 Leaf Trait-LAI Dynamics are Important to C-Cycling Modelling

Our findings align with a growing body of evidence which demonstrates the major role of leaf trait-LAI dynamics in driving regional to global scale variation in C fluxes (Trugman *et al.*, 2019a, Trugman *et al.*, 2019b, Verheijen *et al.*, 2013, Xu *et al.*, 2016). We therefore highlight the importance of concerted efforts to collate canopy aggregated leaf trait data (including LMA, photosynthetic rate, respiration rate, and leaf lifespan) and to record these characteristics through the canopy profile and over full phenological cycles (Lloyd *et al.*, 2010, Meir *et al.*, 2002). Trait data need to be linked to LAI observations and scaled appropriately to understand their economic interactions and sensitivities.

4.7 Limitations

We identify a number of limitations to our results including the absence of leaf age effects, the leaf respiration model used, uncertainty in LAI field estimates and lack of in-situ data on the vertical profile of LAI within the canopy, except at a few tropical forest sites (Meir *et al.*, 2000, Piayda *et*

al., 2015). In addition, we recognise that by not including error associated with all model parameters, nor including model structural error, the C flux uncertainty values presented in our analysis are likely underestimated. In particular our assumption of similar plant hydraulics across sites needs further exploration. These weaknesses can be addressed through concerted modelling and data collection exercises.

We do not simulate a leaf age effect on carboxylation and electron transport rates as to do so would have induced greater uncertainty into our results. Wu *et al.* (2016) suggest that the interaction between leaf age and photosynthetic capacity reported for tropical forests (Kitajima *et al.*, 2002, Kitajima *et al.*, 1997, Xu *et al.*, 2017), drives seasonal C flux dynamics. However, there were insufficient data currently to parameterise the leaf aging process across Amazon trees.

We recognise the limitations of the leaf maintenance respiration model used, namely that though based on biological reasoning, it is an empirical approach (scaling respiration from leaf N content as a function of temperature to estimate respiration), and that tropical trees accounted for only a small proportion of the data used to build the model (Reich *et al.*, 2008). Other models relating leaf N content to respiration rate vary in their parameterisation and form (i.e. linear versus the non-linear Reich model; Atkin et al. 2015, Ryan 1991, Meir 2001). It is vital to improve process modelling of autotrophic respiration, and to find ways to test scaling this leaf process to the canopy, and evaluate its climate sensitivity (Thomas *et al.*, 2019).

While accounting for LAI sampling uncertainty in our results, there is a risk of measurement bias which could shift reported LAI trends, especially at higher leaf area (Bréda, 2003, Jonckheere *et al.*, 2004, Weiss *et al.*, 2004). However, our LAI estimates (from hemispherical photographs) align approximately with destructive sampling measurements from Amazon forests under a similar precipitation regime (Caxiuanã 5.11 ± 1.41 m^2m^{-2}, McWilliam *et al.* (1993), 5.7 ± 0.5 m^2m^{-2}; Araújo et al., 2002; Fisher et al., 2007) so bias effects are unlikely to be large enough to influence our conclusions. In addition, we note that by using linear interpolation to scale monthly LAI estimates to daily values, we may have introduced some uncertainty into our results. However, we expect the effect to be minimal relative to the effect of in-situ LAI estimate uncertainty.

The sensitivity of NCE to differences in the vertical distribution of LAI also remains uncertain. Within SPA the default assumption is to uniformly distribute LAI over the canopy, as done here due to the lack of in-situ information. However, existing analysis of Amazonian forests have

shown that the vertical profile of LAI can deviate significantly from a uniform distribution potentially resulting in significant changes in light absorption and leaf ecophysiological properties (Meir *et al.*, 2000, Stark *et al.*, 2012), as also found in temperature forests (Kull *et al.*, 1999). Stark *et al.* (2012) compared ground based and airborne Lidar estimation of vertical canopy profile of LAI, demonstrating the potential utility of airborne Lidar to resolve this current knowledge gap. An additional complication not yet addressed is that satellite and ground-based Lidar studies have presented evidence of divergent phenologies across different canopy layers (Smith *et al.*, 2019, Tang & Dubayah, 2017).

5. Conclusion

We assessed the potential for optimality-based approaches to improve predictions of tropical LAI and reduce uncertainty in C flux estimates. Our results show that LAI variation across an Amazon-wide moisture stress gradient was optimal in terms of maximising NCE, but that the predictive power of this focused optimisation approach was limited with respect to LAI, as a range of LAI strategies could be equally economically viable. We also demonstrated how different leaf trait strategies can support alternative LAI dynamics. Given the importance of leaf traits in shaping canopy dynamics, we further highlight the importance of mapping spatial, temporal and vertical leaf trait distributions via databases (such as the TRY trait database) and new remote sensing approaches.

Acknowledgements

The authors would like to thank the PhD project funding body, the UK Natural Environment Research Council E3 DTP, NERC, the GHG program GREENHOUSE (NE/K002619/1), the UK's National Centre for Earth Observation (NE/R016518/1), the UKSA project Forests 2020, a Royal Society Wolfson Award to MW, the UK Met Office, the Newton fund, and the CSSP-Brazil project. PM also acknowledges support from NERC grant NE/J011002/1 and ARC grant DP170104091. The TRY trait database is thanked for the data used in model parameterisation and the authors would like to thank the Global Ecosystems Monitoring network team for the field data used in this study, collected through funding from NERC and the Gordon and Betty Moore Foundation, and an ERC Advanced Investigator Award to YM (GEM-TRAIT). In addition, the authors would like to thank the anonymous reviewers for their constructive feedback on the manuscript.

Author Contributions

Sophie Flack-Prain, Mathew Williams and Patrick Meir conceived the research questions. Data used in model calibration and evaluation was collected by Yadvinder Malhi and associates. Model experiments were designed and conducted by Sophie Flack-Prain with contributions from Mathew Williams and Thomas L. Smallman. Sophie Flack-Prain and Mathew Williams prepared the manuscript with active contributions from all co-authors.

Tables

Table 1. Environmental characteristics summary of GEM network Amazon permanent sample plots (Malhi *et al*., 2015). Climate measures including maximum climatological water deficit (MCWD) are derived from local weather station data gap filled with ERA interim data for the years 2009-2010 (Dee *et al*., 2011).

	Caxiuanã Control	**Caxiuanã Tower**	**Tambopata V**	**Tambopata VI**	**Kenia Wet**	**Kenia Dry**	**Tanguro**
RAINFOR site code	CAX04	CAX06	TAM05	TAM06	KEN01	KEN02	---
Latitude (˚N)	-1.716	-1.737	-12.831	-12.839	-16.016	-16.016	-13.077
Longitude (˚E)	-51.457	-51.462	-69.271	-69.296	-62.73	-62.73	52.386
MCWD (mm)	-85.5	-85.5	-256.2	-256.2	-342.3	-342.3	-498.1
Precipitation Seasonality (%)	166.1	166.1	287.9	287.9	391.2	391.2	126.8
Soil type	Vetic Acrisol	Ferralsol	Cambisol	Alisol	Cambisol	Cambisol	Ferralsol
Sand (%)	83.69	32.54	40	2	58.05	55.48	45.73
Clay (%)	10.68	53.76	44	46	19.13	18.25	48.9

Table 2. Mean LAI, LAI seasonality and leaf traits (leaf N content, photosynthetic capacity κ_c, κ_J and LMA) used to parameterise SPA, and SPA calibrated leaf litterfall parameters (leaf fall day, leaf lifespan and leaf fall period) for Amazon permanent sample plots. Leaf fall day is the day of year leaf fall is initiated, leaf lifespan reflects potential lifespan of leaves and leaf fall period is the number of days over which leaf fall occurs. Leaf litterfall parameters were calibrated against GEM field estimates.

	Field Measured Parameters						**Calibrated Parameters**		
	Annual mean LAI (m^2 m^{-2})	LAI Seasonality (%)	Leaf N content (mg g^{-1})	κ_c (μmol C gN^{-1} s^{-1})	κ_J (μmol C gN^{-1} s^{-1})	LMA (g m^{-2})	Leaf Fall Day (day of year)	Leaf Lifespan (years)	Leaf Fall Period (days)
CAX04	5.0	0.2	19.6	15.4	27.7	93.0	210	3	150
CAX06	5.2	2.2	24.3	13.2	23.8	87.4	190	1.45	100
TAM05	4.9	4.9	24.0	28.9	49.9	101.0	220	1.3	130
TAM06	4.6	8.9	24.8	29.0	50.3	96.0	230	1.42	100
KEN01	2.8	14.1	40.4	29.3	51.6	52.5	200	1.05	100
KEN02	2.2	18.4	55.3	28.9	50.3	41.8	180	1.01	100
Tanguro	4.1	1.6	31.2	30.0	53.1	64.4	180	1.04	120

Table 3. Model calibration and evaluation performance for permanent sample plots across an Amazon mean MCWD gradient. SPA forced with observed LAI, calibrated using field estimates of leaf litterfall and soil moisture, and evaluated against annual NPP, GPP and autotrophic respiration. We compare modelled values to field estimates of C fluxes to derive the coefficient of determination, p-value and the normalised root mean square error.

	R^2	p	RMSE(%)
Evaluation			
GPP	0.36	0.15	11.2
R_a	0.59	0.04	12.2
NPP	0.38	0.14	12.0
NCE	0.62	0.04	12.8
Calibration			
Leaf Litterfall	0.99	<0.001	2.8
Litterfall Range	0.54	0.009	23.8
Litterfall Peak Timing	0.96	<0.001	7.1
Soil Moisture Range	0.35	0.21	14.7
Soil Moisture Peak Timing	0.98	<0.001	10.6

Table 4. Linear regression analyses on the interaction between MCWD, precipitation seasonality, and in-situ measurements of mean LAI, LAI seasonality, leaf N content, LMA, and calibrated leaf lifespan across Amazon permanent sample plots.

Interaction	**Slope**	**R^2**	**p-value**
Mean Annual LAI ~ MCWD	+	0.35	0.16
Mean Annual LAI ~ Precipitation Seasonality	-	0.57	0.05
LAI Seasonality ~ MCWD	-	0.13	0.42
LAI Seasonality ~ Precipitation Seasonality	+	0.87	0.002
Mean Annual LAI ~ LAI Seasonality	-	0.79	0.008
LMA ~ MCWD	+	0.37	0.15
LMA ~ Precipitation Seasonality	-	0.23	0.27
LMA ~ Mean Annual LAI	+	0.86	0.002
LMA ~ LAI Seasonality	-	0.49	0.08
LMA ~ Foliar N Content	-	0.85	0.003
LMA ~ Calibrated Leaf Lifespan (log-log)	+	0.39	0.14
Foliar N Content ~ MCWD	-	0.29	0.21
Foliar N Content ~ Precipitation Seasonality	+	0.49	0.08
Foliar N Content ~ Mean Annual LAI	-	0.92	<0.001
Foliar N Content ~ LAI Seasonality	+	0.77	0.009
Foliar N Content ~ Calibrated Leaf Lifespan (log-log)	-	0.57	0.05
Calibrated Leaf Lifespan ~ MCWD	+	0.49	0.08
Calibrated Leaf Lifespan ~ Precipitation Seasonality	-	0.20	0.31
Calibrated Leaf Lifespan ~ Mean Annual LAI	+	0.28	0.23
Calibrated Leaf Lifespan ~ LAI Seasonality	-	0.30	0.20

Figure Legends

Figure 1. Hypothesised GPP, NCE and leaf growth and maintenance C-costs across a mean LAI gradient for a typical low and high moisture-stress plot. Optimal LAI is lower for high moisture-stress plots, due the effect of water limitation on stomatal conductance, consequently limiting GPP and NCE at higher leaf area. GPP and NCE increase with mean LAI for low moisture-stress plots as water constraints to stomatal conductance are lower.

Figure 2. A summary of the pathways through which key leaf-level traits, LAI time-series (LAI_t), meteorology, and soil properties constrain C and water fluxes in SPA. Model inputs derived from field measurements are presented in red. Dashed boxes identify model calibrated values. Green dotted circles highlight model values which determine total C assimilation, the C cost of leaf growth and maintenance, and phenology (where NCE = GPP – NPP_{Leaf} – RM_{Leaf} - RG_{Leaf}). The joining together of multiple arrows indicates a collective impact. C_{Leaf} = leaf C stock; NPP_{Leaf} = leaf net primary productivity; $Litterfall_{Leaf}$ = leaf litterfall; RG_{Leaf} = leaf growth respiration; RM_{Leaf} = leaf maintenance respiration; NPP_{Total} = total net primary productivity; NPP_{Root} = fine root net primary productivity; C_{Root} = fine root C stock; GPP= gross primary productivity; LMA= leaf mass per unit area; κ_c & κ_j = V_{cmax} and J_{max} normalised by leaf nitrogen content respectively (i.e. photosynthetic capacity); leaf N = leaf nitrogen content.

Figure 3. Field estimated monthly LAI, leaf litterfall (GEM), and standard error, compared with SPA simulated leaf litterfall for seven plots at four locations across the Amazon basin. SPA leaf litterfall was calibrated against GEM estimates to derive three fixed model drivers relating to the leaf cycle (peak leaf fall timing, leaf fall period and leaf lifespan). GEM leaf litterfall data was available for 2009-2010 for CAX04, CAX06, TAM05, TAM06 and for 2010 only for KEN01, KEN02 and Tanguro. R^2, p-value and RMSE estimates presented are derived from linear regressions between monthly GEM measurements and SPA simulations.

Figure 4. Model simulated NCE, GPP, and leaf growth and maintenance C-costs, for each plot along an Amazon MCWD gradient, forced with synthetic LAI timeseries ranging in mean LAI. Data points are field estimates of NCE, GPP, and leaf growth and maintenance. Error bars show the propagated error of summed components.

Figure 5. The interaction between MCWD and simulated optimal (i.e. that which maximises NCE) and observed (i.e. field measured) mean annual LAI (a) and LAI seasonality (b).

Figure 6. A comparison of maximum simulated NCE forced with synthetic LAI timeseries ranging in mean LAI against (a) field estimated NCE, and (b) SPA simulated NCE under nominal LAI. SPA error bars represent simulated NCE and GPP under field measured LAI standard error. GEM error bars represent propagated error for summed field estimates of component NPP and respiration. The dashed line is the 1:1 and the solid line is the linear regression between NCE estimates.

Figure 7. Model simulated NCE, GPP, and leaf growth and maintenance, for each plot along an Amazon MCWD gradient, forced with synthetic LAI timeseries ranging in LAI seasonality. Data points are field estimates of NCE, GPP, and leaf growth and maintenance. Error bars show the propagated error of summed components.

Figure 8. Simulated NCE for Amazon forest plots under low (CAX04) and high (KEN02) moisture-stress, forced with synthetic LAI timeseries ranging in mean LAI (top panels) and LAI seasonality (bottom panels) under fast (black) and slow (blue) leaf traits. Data points are field estimates of mean LAI/LAI seasonality and NCE. Vertical error bars show the propagated error of summed components. Horizontal error bars show LAI standard error.

Data Sharing and Accessibility

The data that support the findings of this study are openly available in Edinburgh DataShare at https://doi.org/10.7488/ds/2925, reference number 10283/3761.

References

Abelho M, Cressa C, Graça MaS (2005) Microbial Biomass, Respiration, and Decomposition of Hura crepitans L.(Euphorbiaceae) Leaves in a Tropical Stream 1. Biotropica: The Journal of Biology and Conservation, 37, 397-402. doi: 10.1111/j.1744-7429.2005.00052.x

Ackerly D (1999) Self-shading, carbon gain and leaf dynamics: a test of alternative optimality models. Oecologia, 119, 300-310. doi: 10.1007/s004420050790

Amthor JS, Goulden ML, Munger JW, Wofsy SC (1994) Testing a mechanistic model of forest-canopy mass and energy exchange using eddy correlation: carbon dioxide and ozone uptake by a mixed oak-maple stand. Functional Plant Biology, 21, 623-651. doi: 10.1071/PP9940623

Anten NPR (2016) Optimization and game theory in canopy models. In: Canopy photosynthesis: from basics to applications. pp 355-377, Springer. doi: 10.1007/978-94-017-7291-4_13

Anten NPR, During HJ (2011) Is analysing the nitrogen use at the plant canopy level a matter of choosing the right optimization criterion? Oecologia, 167, 293-303. doi: 10.1007/s00442-011-2011-3

Aragao LEOC, Malhi Y, Metcalfe DB, Silva-Espejo JE, Jimenez E, Navarrete D, Almeida S, Costa ACL, Salinas N, Phillips OL, Anderson LO, Alvarez E, Baker TR, Goncalvez PH, Huaman-Ovalle J, Mamani-Solorzano M, Meir P, Monteagudo A, Patino S, Penuela MC, Prieto A, Quesada CA, Rozas-Davila A, Rudas A, Silva JA, Vasquez R (2009) Above- and below-ground net primary productivity across ten Amazonian forests on contrasting soils. Biogeosciences, 6, 2759-2778. doi: 10.5194/bg-6-2759-2009

Araujo-Murakami A, Doughty CE, Metcalfe DB, Silva-Espejo JE, Arroyo L, Heredia JP, Flores M, Sibler R, Mendizabal LM, Pardo-Toledo E, Vega M, Moreno L, Rojas-Landivar VD, Halladay K, Girardin CaJ, Killeen TJ, Malhi Y (2014) The productivity, allocation and cycling of carbon in forests at the dry margin of the Amazon forest in Bolivia. Plant Ecology & Diversity, 7, 55-69. doi: 10.1080/17550874.2013.798364

Araújo AC, Nobre AD, Kruijt B, Elbers JA, Dallarosa R, Stefani P, Von Randow C, Manzi AO, Culf AD, Gash JHC (2002) Comparative measurements of carbon dioxide fluxes from two nearby towers in a central Amazonian rainforest: The Manaus LBA site. Journal of Geophysical Research: Atmospheres, 107, LBA-58. doi: 10.1029/2001JD000676

Atkin OK, Bloomfield KJ, Reich PB, Tjoelker MG, Asner GP, Bonal D, Bönisch G, Bradford MG, Cernusak LA, Cosio EG (2015) Global variability in leaf respiration in relation to climate, plant functional types and leaf traits. New Phytologist, 206, 614-636. doi: 10.1111/nph.13253

Baldocchi D, Valentini R, Running S, Oechel W, Dahlman R (1996) Strategies for measuring and modelling carbon dioxide and water vapour fluxes over terrestrial ecosystems. Global Change Biology, 2, 159-168. doi: 10.1111/j.1365-2486.1996.tb00069.x

Bloom AA, Williams M (2015) Constraining ecosystem carbon dynamics in a data-limited world: integrating ecological "common sense" in a model-data fusion framework. Biogeosciences, 12, 1299-1315. doi: 10.5194/bg-12-1299-2015

Bonan GB, Williams M, Fisher RA, Oleson KW (2014) Modeling stomatal conductance in the earth system: linking leaf water-use efficiency and water transport along the soil–plant–atmosphere continuum. Geoscientific Model Development, 7, 2193-2222. doi: 10.5194/gmdd-7-3085-2014

Braghiere RK, Quaife T, Black E, He L, Chen JM (2019) Underestimation of global photosynthesis in Earth System Models due to representation of vegetation structure. Global Biogeochemical Cycles, 33, 1358-1369. doi: 10.1029/2018GB006135

Bréda NJJ (2003) Ground-based measurements of leaf area index: a review of methods, instruments and current controversies. Journal of experimental botany, 54, 2403-2417. doi: 10.1093/jxb/erg263

Caldararu S, Palmer PI, Purves DW (2012) Inferring Amazon leaf demography from satellite observations of leaf area index. Biogeosciences, 9, 1389-1404. doi: 10.5194/bg-9-1389-2012

Caldararu S, Purves DW, Palmer PI (2014) Phenology as a strategy for carbon optimality: a global model. Biogeosciences, 11, 763-778. doi: 10.5194/bg-11-763-2014

Caldararu S, Purves DW, Smith MJ (2016) The effect of using the plant functional type paradigm on a data-constrained global phenology model. Biogeosciences, 13, 925-941. doi: 10.5194/bg-13-925-2016

Carswell FE, Costa AL, Palheta M, Malhi Y, Meir P, Costa JDR, Ruivo MD, Leal LDM, Costa JMN, Clement RJ, Grace J (2002) Seasonality in CO_2 and H_2O flux at an eastern Amazonian rain forest. Journal of Geophysical Research-Atmospheres, 107. doi: 10.1029/2000JD000284

Carswell FE, Meir P, Wandelli EV, Bonates LCM, Kruijt B, Barbosa EM, Nobre AD, Grace J, Jarvis PG (2000) Photosynthetic capacity in a central Amazonian rain forest. Tree Physiology, 20, 179-186. doi: 10.1093/treephys/20.3.179

Chave J, Navarrete D, Almeida S, Álvarez E, Aragão LEOC, Bonal D, Châtelet P, Silva-Espejo JE, Goret JY, Von Hildebrand P (2010) Regional and seasonal patterns of litterfall in tropical South America. Biogeosciences, 7, 43-55. doi: 10.5194/bg-7-43-2010

Clark DB, Mercado LM, Sitch S, Jones CD, Gedney N, Best MJ, Pryor M, Rooney GG, Essery RLH, Blyth E (2011) The Joint UK Land Environment Simulator (JULES), model description–

Part 2: carbon fluxes and vegetation dynamics. Geoscientific Model Development, 4, 701-722. doi: 10.5194/gmd-4-701-2011

Davies SJ, Tan S, Lafrankie JV, Potts MD (2005) Soil-related floristic variation in a hyperdiverse dipterocarp forest. In: Pollination ecology and the rain forest. pp 22-34, Springer.

De Kauwe MG, Medlyn BE, Zaehle S, Walker AP, Dietze MC, Wang YP, Luo Y, Jain AK, El-Masri B, Hickler T (2014) Where does the carbon go? A model–data intercomparison of vegetation carbon allocation and turnover processes at two temperate forest free-air CO_2 enrichment sites. New Phytologist, 203, 883-899. doi: 10.1111/nph.12847

De Weirdt M, Verbeeck H, Maignan F, Peylin P, Poulter B, Bonal D, Ciais P, Steppe K (2012) Seasonal leaf dynamics for tropical evergreen forests in a process-based global ecosystem model. Geoscientific Model Development, 5, 1091-1108. doi: 10.5194/gmd-5-1091-2012

Dee DP, Uppala SM, Simmons AJ, Berrisford P, Poli P, Kobayashi S, Andrae U, Balmaseda MA, Balsamo G, Bauer P (2011) The ERA-Interim reanalysis: Configuration and performance of the data assimilation system. Quarterly Journal of the royal meteorological society, 137, 553-597. doi: 10.1002/qj.828

Demarez V, Duthoit S, Baret F, Weiss M, Dedieu G (2008) Estimation of leaf area and clumping indexes of crops with hemispherical photographs. Agricultural and Forest Meteorology, 148, 644-655. doi: 10.1016/j.agrformet.2007.11.015

Dewar RC, Franklin O, Mäkelä A, Mcmurtrie RE, Valentine HT (2009) Optimal function explains forest responses to global change. Bioscience, 59, 127-139. doi: 10.1525/bio.2009.59.2.6

Doughty CE, Metcalfe DB, Girardin CA, Amezquita FF, Cabrera DG, Huasco WH, Silva-Espejo JE, Araujo-Murakami A, Da Costa MC, Rocha W, Feldpausch TR, Mendoza AL, Da Costa AC, Meir P, Phillips OL, Malhi Y (2015) Drought impact on forest carbon dynamics and fluxes in Amazonia. Nature, 519, 78-82. doi: 10.1038/nature14213

Evans JR (1989) Photosynthesis and nitrogen relationships in leaves of C 3 plants. Oecologia, 78, 9-19. doi: 10.1007/BF00377192

Farquhar GD, Von Caemmerer S (1982) Modelling of photosynthetic response to environmental conditions. In: Physiological plant ecology II. pp 549-587, Springer. doi: 10.1007/978-3-642-68150-9_17

Field C (1983) Allocating leaf nitrogen for the maximization of carbon gain: leaf age as a control on the allocation program. Oecologia, 56, 341-347. doi: 10.1007/BF00379710

Figueroa-Esquivel E, Puebla-Olivares F, Godínez-Álvarez H, Núñez-Farfán J (2009) Seed dispersal effectiveness by understory birds on Dendropanax arboreus in a fragmented landscape. Biodiversity and Conservation, 18, 3357-3365. doi: 10.1007/s10531-009-9645-z

Fisher JB, Badgley G, Blyth E (2012) Global nutrient limitation in terrestrial vegetation. Global Biogeochemical Cycles, 26, 3. doi: 10.1029/2011GB004252

Fisher RA, Williams M, Da Costa AL, Malhi Y, Da Costa RF, Almeida S, Meir P (2007) The response of an Eastern Amazonian rain forest to drought stress: results and modelling analyses from a throughfall exclusion experiment. Global Change Biology, 13, 2361-2378. doi: 10.1111/j.1365-2486.2007.01417.x

Fisher RA, Williams M, Do V, Lobo R, Da Costa AL, Meir P (2006) Evidence from Amazonian forests is consistent with isohydric control of leaf water potential. Plant, Cell & Environment, 29, 151-165. doi: 10.1111/j.1365-3040.2005.01407.x

Flack-Prain S, Meir P, Malhi Y, Smallman TL, Williams M (2019) The importance of physiological, structural and trait responses to drought stress in driving spatial and temporal variation in GPP across Amazon forests. Biogeosciences, 16, 4463-4484. doi: 10.5194/bg-16-4463-2019

Franklin O, Mcmurtrie R, Iversen CM, Crous KY, Finzi AC, Tissue DT, Ellsworth DS, Oren RaM, Norby RJ (2009) Forest fine-root production and nitrogen use under elevated CO_2: contrasting responses in evergreen and deciduous trees explained by a common principle. Global Change Biology, 15, 132-144. doi: 10.1111/j.1365-2486.2008.01710.x

Fyllas NM, Patino S, Baker TR, Nardoto GB, Martinelli LA, Quesada CA, Paiva R, Schwarz M, Horna V, Mercado LM, Santos A, Arroyo L, Jimenez EM, Luizao FJ, Neill DA, Silva N, Prieto A, Rudas A, Silviera M, Vieira ICG, Lopez-Gonzalez G, Malhi Y, Phillips OL, Lloyd J (2009) Basin-

wide variations in foliar properties of Amazonian forest: phylogeny, soils and climate. Biogeosciences, 6, 2677-2708. doi: 10.5194/bg-6-2677-2009

Geber MA, Griffen LR (2003) Inheritance and natural selection on functional traits. International Journal of Plant Sciences, 164, S21-S42. doi: 1058-5893/2003/16403S-0003

Givnish TJ (2002) Adaptive significance of evergreen vs. deciduous leaves: solving the triple paradox. Silva fennica, 36, 703-743.

Grier CC, Running SW (1977) Leaf Area of Mature Northwestern Coniferous Forests - Relation to Site Water-Balance. Ecology, 58, 893-899. doi: 10.2307/1936225

Haverd V, Smith B, Raupach MR, Briggs PR, Nieradzik LP, Beringer J, Hutley LB, Trudinger CM, Cleverly J (2016) Coupling carbon allocation with leaf and root phenology predicts tree-grass partitioning along a savanna rainfall gradient. Biogeosciences, 761-779. doi: 10.5194/bg-13-761-2016

Iio A, Hikosaka K, Anten NPR, Nakagawa Y, Ito A (2014) Global dependence of field-observed leaf area index in woody species on climate: a systematic review. Global Ecology and Biogeography, 23, 274-285. doi: 10.1111/geb.12133

Ito E, Khorn S, Lim S, Pol S, Tith B, Pith P, Tani A, Kanzaki M, Kaneko T, Okuda Y, Kabeya N, Nobuhiro T, Araki M (2007) Comparison of the Leaf Area Index (LAI) of Two Types of Dipterocarp Forest on the West Bank of the Mekong River, Cambodia. In: Forest Environments in the Mekong River Basin. (eds Sawada H, Araki M, Chappell NA, Lafrankie JV, Shimizu A) pp 214-221, Tokyo, Springer Japan. doi: 10.1007/978-4-431-46503-4_19

Jolly WM, Nemani R, Running SW (2005) A generalized, bioclimatic index to predict foliar phenology in response to climate. Global Change Biology, 11, 619-632. doi: 10.1111/j.1365-2486.2005.00930.x

Jonckheere I, Fleck S, Nackaerts K, Muys B, Coppin P, Weiss M, Baret F (2004) Review of methods for in situ leaf area index determination - Part I. Theories, sensors and hemispherical photography. Agricultural and Forest Meteorology, 121, 19-35. doi: 10.1016/j.agrformet.2003.08.027

Jones S, Rowland L, Cox P, Hemming D, Wiltshire A, Williams K, Parazoo NC, Liu J, Da Costa ACL, Meir P (2019) The Impact of a Simple Representation of Non-Structural Carbohydrates on the Simulated Response of Tropical Forests to Drought. Biogeosciences Discussions, 1-26. doi: 10.5194/bg-17-3589-2020

Kikuzawa K (1991) A cost-benefit analysis of leaf habit and leaf longevity of trees and their geographical pattern. The American Naturalist, 138, 1250-1263. doi: 10.1086/285281

Kikuzawa K (1996) Geographical distribution of leaf life span and species diversity of trees simulated by a leaf-longevity model. Vegetation, 122, 61-67. doi: 10.1007/BF00052816

Kim Y, Knox RG, Longo M, Medvigy D, Hutyra LR, Pyle EH, Wofsy SC, Bras RL, Moorcroft PR (2012) Seasonal carbon dynamics and water fluxes in an Amazon rainforest. Global Change Biology, 18, 1322-1334. doi: 10.1111/j.1365-2486.2011.02629.x

Kitajima K, Mulkey SS, Samaniego M, Joseph Wright S (2002) Decline of photosynthetic capacity with leaf age and position in two tropical pioneer tree species. American Journal of Botany, 89, 1925-1932. doi: 10.3732/ajb.89.12.1925

Kitajima K, Mulkey SS, Wright SJ (1997) Decline of photosynthetic capacity with leaf age in relation to leaf longevities for five tropical canopy tree species. American Journal of Botany, 84, 702-708. doi: 10.2307/2445906

Kull O, Broadmeadow M, Kruijt B, Meir P (1999) Light distribution and foliage structure in an oak canopy. Trees, 14, 55-64. doi: 10.1007/s004680050209

Kumagai T, Ichie T, Yoshimura M, Yamashita M, Kenzo T, Saitoh TM, Ohashi M, Suzuki M, Koike T, Komatsu H (2006) Modeling CO_2 exchange over a Bornean tropical rain forest using measured vertical and horizontal variations in leaf-level physiological parameters and leaf area densities. Journal of Geophysical Research: Atmospheres, 111, D10. doi: 10.1029/2005JD006676

Liu J, Bowman KW, Schimel DS, Parazoo NC, Jiang Z, Lee M, Bloom AA, Wunch D, Frankenberg C, Sun Y (2017) Contrasting carbon cycle responses of the tropical continents to the 2015–2016 El Niño. Science, 358, 6360. doi: 10.1126/science.aam5690

Liu Y, Xiao J, Ju W, Zhu G, Wu X, Fan W, Li D, Zhou Y (2018) Satellite-derived LAI products exhibit large discrepancies and can lead to substantial uncertainty in simulated carbon and water fluxes. Remote sensing of Environment, 206, 174-188. doi: 10.1016/j.rse.2017.12.024

Lloyd J, Patiño S, Paiva RQ, Nardoto GB, Quesada CA, Santos AJB, Baker TR, Brand WA, Hilke I, Gielmann H (2010) Optimisation of photosynthetic carbon gain and within-canopy gradients of associated foliar traits for Amazon forest trees. Biogeosciences, 7, 1833-1859. doi: 10.5194/bg-7-1833-2010

López-Blanco E, Lund M, Williams M, Tamstorf M P, Westergaard-Nielsen A, Exbrayat J-F, Hansen BU, Christensen T R (2017) Exchange of CO_2 in Arctic tundra: impacts of meteorological variations and biological disturbance. Biogeosciences, 14, 4467–4483. doi: 10.5194/bg-14-4467-2017

Malhi Y, Amezquita FF, Doughty CE, Silva-Espejo JE, Girardin CaJ, Metcalfe DB, Aragao LEOC, Huaraca-Quispe LP, Alzamora-Taype I, Eguiluz-Mora L, Marthews TR, Halladay K, Quesada CA, Robertson AL, Fisher JB, Zaragoza-Castells J, Rojas-Villagra CM, Pelaez-Tapia Y, Salinas N, Meir P, Phillips OL (2014) The productivity, metabolism and carbon cycle of two lowland tropical forest plots in south-western Amazonia, Peru. Plant Ecology & Diversity, 7, 85-105. doi: 10.1080/17550874.2013.820805

Malhi Y, Doughty CE, Goldsmith GR, Metcalfe DB, Girardin CaJ, Marthews TR, Del Aguila-Pasquel J, Aragao LEOC, Araujo-Murakami A, Brando P, Da Costa ACL, Silva-Espejo JE, Amezquita FF, Galbraith DR, Quesada CA, Rocha W, Salinas-Revilla N, Silverio D, Meir P, Phillips OL (2015) The linkages between photosynthesis, productivity, growth and biomass in lowland Amazonian forests. Global Change Biology, 21, 2283-2295. doi: 10.1111/gcb.12859

Malhi Y, Roberts JT, Betts RA, Killeen TJ, Li W, Nobre CA (2008) Climate change, deforestation, and the fate of the Amazon. Science, 319, 169-72. doi: 10.1126/science.1146961

Mcmurtrie RE, Dewar RC (2011) Leaf-trait variation explained by the hypothesis that plants maximize their canopy carbon export over the lifespan of leaves. Tree Physiology, 31, 1007-1023. doi: 10.1093/treephys/tpr037

Mcmurtrie RE, Norby RJ, Medlyn BE, Dewar RC, Pepper DA, Reich PB, Barton CVM (2008) Why is plant-growth response to elevated CO_2 amplified when water is limiting, but reduced when

nitrogen is limiting? A growth-optimisation hypothesis. Functional Plant Biology, 35, 521-534. doi: 10.1071/FP08128

Mcwilliam AL, Roberts JM, Cabral OMR, Leitao M, De Costa ACL, Maitelli GT, Zamparoni C (1993) Leaf area index and above-ground biomass of terra firme rain forest and adjacent clearings in Amazonia. Functional ecology, 310-317. doi: 10.2307/2390210

Meir P, Grace J, Miranda AC (2000) Photographic method to measure the vertical distribution of leaf area density in forests. Agricultural and Forest Meteorology, 102, 105-111. doi: 10.1016/S0168-1923(00)00122-2

Meir P, Grace J, Miranda AC (2001) Leaf respiration in two tropical rainforests: constraints on physiology by phosphorus, nitrogen and temperature. Functional ecology, 15, 378-387. doi: 10.1046/j.1365-2435.2001.00534.x

Meir P, Kruijt B, Broadmeadow M, Barbosa E, Kull O, Carswell F, Nobre A, Jarvis PG (2002) Acclimation of photosynthetic capacity to irradiance in tree canopies in relation to leaf nitrogen concentration and leaf mass per unit area. Plant, Cell & Environment, 25, 343-357. doi: 10.1046/j.0016-8025.2001.00811.x

Metcalfe DB, Meir P, Aragão LEOC, Lobo-Do-Vale R, Galbraith D, Fisher RA, Chaves MM, Maroco JP, Da Costa ACL, De Almeida SS (2010) Shifts in plant respiration and carbon use efficiency at a large-scale drought experiment in the eastern Amazon. New Phytologist, 187, 608-621. doi: 10.1111/j.1469-8137.2010.03319.x

Muraoka H, Saigusa N, Nasahara KN, Noda H, Yoshino J, Saitoh TM, Nagai S, Murayama S, Koizumi H (2010) Effects of seasonal and interannual variations in leaf photosynthesis and canopy leaf area index on gross primary production of a cool-temperate deciduous broadleaf forest in Takayama, Japan. Journal of plant research, 123, 563-576. doi: 10.1007/s10265-009-0270-4

Myneni RB, Yang W, Nemani RR, Huete AR, Dickinson RE, Knyazikhin Y, Didan K, Fu R, Negron Juarez RI, Saatchi SS, Hashimoto H, Ichii K, Shabanov NV, Tan B, Ratana P, Privette JL, Morisette JT, Vermote EF, Roy DP, Wolfe RE, Friedl MA, Running SW, Votava P, El-Saleous N, Devadiga S, Su Y, Salomonson VV (2007) Large seasonal swings in leaf area of Amazon rainforests. Proc Natl Acad Sci U S A, 104, 4820-3. doi: 10.1073/pnas.0611338104

Pan Y, Birdsey RA, Fang J, Houghton R, Kauppi PE, Kurz WA, Phillips OL, Shvidenko A, Lewis SL, Canadell JG (2011) A large and persistent carbon sink in the world's forests. Science, 333, 988-993. doi: 10.1126/science.1201609

Piayda A, Dubbert M, Werner C, Correia AV, Pereira JS, Cuntz M (2015) Influence of woody tissue and leaf clumping on vertically resolved leaf area index and angular gap probability estimates. Forest Ecology and Management, 340, 103-113. doi: 10.1016/j.foreco.2014.12.026

Poorter L, Bongers F (2006) Leaf traits are good predictors of plant performance across 53 rain forest species. Ecology, 87, 1733-1743. doi: 10.1890/0012-9658(2006)87[1733:LTAGPO]2.0.CO;2

Quesada CA, Lloyd J, Schwarz M, Patino S, Baker TR, Czimczik C, Fyllas NM, Martinelli L, Nardoto GB, Schmerler J, Santos AJB, Hodnett MG, Herrera R, Luizao FJ, Arneth A, Lloyd G, Dezzeo N, Hilke I, Kuhlmann I, Raessler M, Brand WA, Geilmann H, Moraes JO, Carvalho FP, Araujo RN, Chaves JE, Cruz OF, Pimentel TP, Paiva R (2010) Variations in chemical and physical properties of Amazon forest soils in relation to their genesis. Biogeosciences, 7, 1515-1541. doi: 10.5194/bg-7-1515-2010.

Quesada CA, Phillips OL, Schwarz M, Czimczik CI, Baker TR, Patino S, Fyllas NM, Hodnett MG, Herrera R, Almeida S, Davila EA, Arneth A, Arroyo L, Chao KJ, Dezzeo N, Erwin T, Di Fiore A, Higuchi N, Coronado EH, Jimenez EM, Killeen T, Lezama AT, Lloyd G, Lopez-Gonzalez G, Luizao FJ, Malhi Y, Monteagudo A, Neill DA, Vargas PN, Paiva R, Peacock J, Penuela MC, Cruz AP, Pitman N, Priante N, Prieto A, Ramirez H, Rudas A, Salomao R, Santos AJB, Schmerler J, Silva N, Silveira M, Vasquez R, Vieira I, Terborgh J, Lloyd J (2012) Basin-wide variations in Amazon forest structure and function are mediated by both soils and climate. Biogeosciences, 9, 2203-2246. doi: 10.5194/bg-9-2203-2012.

Reich PB, Falster DS, Ellsworth DS, Wright IJ, Westoby M, Oleksyn J, Lee TD (2009) Controls on declining carbon balance with leaf age among 10 woody species in Australian woodland: do leaves have zero daily net carbon balances when they die? New Phytologist, 183, 153-166. doi: 10.1111/j.1469-8137.2009.02824.x

Reich PB, Tjoelker MG, Pregitzer KS, Wright IJ, Oleksyn J, Machado JL (2008) Scaling of respiration to nitrogen in leaves, stems and roots of higher land plants. Ecol Lett, 11, 793-801. doi: 10.1111/j.1461-0248.2008.01185.x

Reich PB, Uhl C, Walters MB, Ellsworth DS (1991) Leaf lifespan as a determinant of leaf structure and function among 23 Amazonian tree species. Oecologia, 86, 16-24. doi: 10.1007/BF00317383

Restrepo-Coupe N, Levine NM, Christoffersen BO, Albert LP, Wu J, Costa MH, Galbraith D, Imbuzeiro H, Martins G, Araujo AC (2017) Do dynamic global vegetation models capture the seasonality of carbon fluxes in the Amazon basin? A data-model intercomparison. Global Change Biology, 23, 191-208. doi: 10.1111/gcb.13442

Rocha W, Metcalfe DB, Doughty CE, Brando P, Silvério D, Halladay K, Nepstad DC, Balch JK, Malhi Y (2014) Ecosystem productivity and carbon cycling in intact and annually burnt forest at the dry southern limit of the Amazon rainforest (Mato Grosso, Brazil). Plant Ecology & Diversity, 7, 25-40. doi: 10.1080/17550874.2013.798368

Rowland L, Harper A, Christoffersen BO, Galbraith DR, Imbuzeiro HMA, Powell TL, Doughty C, Levine NM, Malhi Y, Saleska SR, Moorcroft PR, Meir P, Williams M (2015a) Modelling climate change responses in tropical forests: similar productivity estimates across five models, but different mechanisms and responses. Geoscientific Model Development, 8, 1097-1110. doi: 10.5194/gmd-8-1097-2015

Rowland L, Lobo-Do-Vale RL, Christoffersen BO, Melém EA, Kruijt B, Vasconcelos SS, Domingues T, Binks OJ, Oliveira AaR, Metcalfe D (2015b) After more than a decade of soil moisture deficit, tropical rainforest trees maintain photosynthetic capacity, despite increased leaf respiration. Global Change Biology, 21, 4662-4672. doi: 10.1111/gcb.13035

Ryan MG (1991) Effects of climate change on plant respiration. Ecological Applications, 1, 157-167. doi: 10.2307/1941808

Sakschewski B, Von Bloh W, Boit A, Rammig A, Kattge J, Poorter L, Peñuelas J, Thonicke K (2015) Leaf and stem economics spectra drive diversity of functional plant traits in a dynamic global vegetation model. Global Change Biology, 21, 2711-2725. doi: 10.1111/gcb.12870

Saxton KE, Rawls WJ, Romberger JS, Papendick RI (1986) Estimating generalized soil-water characteristics from texture. Soil Science Society of America Journal, 50, 1031-1036. doi: 10.2136/sssaj1986.03615995005000040039x

Schleppi P, Thimonier A, Walthert L (2011) Estimating leaf area index of mature temperate forests using regressions on site and vegetation data. Forest Ecology and Management, 261, 601-610. doi: 10.1016/j.foreco.2010.11.013

Sellers PJ, Dickinson RE, Randall DA, Betts AK, Hall FG, Berry JA, Collatz GJ, Denning AS, Mooney HA, Nobre CA (1997) Modeling the exchanges of energy, water, and carbon between continents and the atmosphere. Science, 275, 502-509. doi: 10.1126/science.275.5299.502

Smallman TL, Moncrieff JB, Williams M (2013) WRFv3. 2-SPAv2: development and validation of a coupled ecosystem–atmosphere model, scaling from surface fluxes of CO_2 and energy to atmospheric profiles. Geoscientific Model Development, 6, 1079-1093. doi: :10.5194/gmdd-6-1559-2013

Smith MN, Stark SC, Taylor TC, Ferreira ML, De Oliveira E, Restrepo-Coupe N, Chen S, Woodcock T, Dos Santos DB, Alves LF (2019) Seasonal and drought-related changes in leaf area profiles depend on height and light environment in an Amazon forest. New Phytologist, 222, 1284-1297. doi: 10.1111/nph.15726

Stark SC, Leitold V, Wu JL, Hunter MO, De Castilho CV, Costa FRC, Mcmahon SM, Parker GG, Shimabukuro MT, Lefsky MA (2012) Amazon forest carbon dynamics predicted by profiles of canopy leaf area and light environment. Ecology letters, 15, 1406-1414. doi: 10.1111/j.1461-0248.2012.01864.x

Street LE, Shaver GR, Williams M, Van Wijk MT (2007) What is the relationship between changes in canopy leaf area and changes in photosynthetic CO_2 flux in arctic ecosystems? Journal of ecology, 95, 139-150. doi: 10.1111/j.1365-2745.2006.01187.x

Sus O, Williams M, Bernhofer C, Béziat P, Buchmann N, Ceschia E, Doherty R, Eugster W, Grünwald T, Kutsch W, Smith P (2010) A linked carbon cycle and crop developmental model: Description and evaluation against measurements of carbon fluxes and carbon stocks at several European agricultural sites. Agriculture, Ecosystems & Environment, 139, 402–418. doi: 10.1016/j.agee.2010.06.012

Tang H, Dubayah R (2017) Light-driven growth in Amazon evergreen forests explained by seasonal variations of vertical canopy structure. Proceedings of the National Academy of Sciences, 114, 2640-2644. doi: 10.1073/pnas.1616943114

Thomas RQ, Williams M (2014) A model using marginal efficiency of investment to analyze carbon and nitrogen interactions in terrestrial ecosystems. doi: 10.5194/gmd-7-2015-2014

Thomas RQ, Williams M, Cavaleri MA, Exbrayat JF, Smallman TL, Street LE (2019) Alternate trait-based leaf respiration schemes evaluated at ecosystem-scale through carbon optimization modeling and canopy property data. Journal of Advances in Modeling Earth Systems. doi: 10.1029/2019MS001679

Thornton PE, Zimmermann NE (2007) An improved canopy integration scheme for a land surface model with prognostic canopy structure. Journal of Climate, 20, 3902-3923. doi: 10.1175/JCLI4222.1

Trugman AT, Anderegg LDL, Sperry JS, Wang Y, Venturas M, Anderegg WRL (2019a) Leveraging plant hydraulics to yield predictive and dynamic plant leaf allocation in vegetation models with climate change. Global Change Biology, 12, 4008-4021. doi: 10.1111/gcb.14814

Trugman AT, Anderegg LDL, Wolfe BT, Birami B, Ruehr NK, Detto M, Bartlett MK, Anderegg WRL (2019b) Climate and plant trait strategies determine tree carbon allocation to leaves and mediate future forest productivity. Global Change Biology, 10, 3395-3405. doi: 10.1111/gcb.14680

Van Loon MP, Schieving F, Rietkerk M, Dekker SC, Sterck F, Anten NPR (2014) How light competition between plants affects their response to climate change. New Phytologist, 203, 1253-1265. doi: 10.1111/nph.12865

Verheijen LM, Brövkin V, Aerts R, Bonisch G, Cornelissen JH, Kattge J, Reich PB, Wright IJ, Van Bodegom PM (2013) Impacts of trait variation through observed trait-climate relationships on performance of an Earth system model: a conceptual analysis. Biogeosciences, 10, 5497–5515. doi: 10.5194/bg-10-5497-2013

Vico G, Dralle D, Feng X, Thompson S, Manzoni S (2017) How competitive is drought deciduousness in tropical forests? A combined eco-hydrological and eco-evolutionary approach. Environmental Research Letters, 12, 065006. doi:10.1088/1748-9326/aa6f1b

Violle C, Navas ML, Vile D, Kazakou E, Fortunel C, Hummel I, Garnier E (2007) Let the concept of trait be functional! Oikos, 116, 882-892. doi: 10.1111/j.0030-1299.2007.15559.x

Walker AP, Beckerman AP, Gu L, Kattge J, Cernusak LA, Domingues TF, Scales JC, Wohlfahrt G, Wullschleger SD, Woodward FI (2014a) The relationship of leaf photosynthetic traits–Vcmax and Jmax–to leaf nitrogen, leaf phosphorus, and specific leaf area: a meta-analysis and modeling study. Ecology and evolution, 4, 3218-3235. doi: 10.1002/ece3.1173

Walker AP, Hanson PJ, De Kauwe MG, Medlyn BE, Zaehle S, Asao S, Dietze M, Hickler T, Huntingford C, Iversen CM (2014b) Comprehensive ecosystem model-data synthesis using multiple data sets at two temperate forest free-air CO_2 enrichment experiments: Model performance at ambient CO_2 concentration. Journal of Geophysical Research: Biogeosciences, 119, 937-964. doi: 10.1002/2013JG002553

Waring RH, Schlesinger WH (1985) Forest ecosystems. Concepts and management, Academic Press.

Weiss M, Baret F, Smith GJ, Jonckheere I, Coppin P (2004) Review of methods for in situ leaf area index (LAI) determination Part II. Estimation of LAI, errors and sampling. Agricultural and Forest Meteorology, 121, 37-53. doi: 10.1016/j.agrformet.2003.08.001

Williams M, Bond BJ, Ryan MG (2001) Evaluating different soil and plant hydraulic constraints on tree function using a model and sap flow data from ponderosa pine. Plant, Cell & Environment, 24, 679-690. doi: 10.1046/j.1365-3040.2001.00715.x

Williams M, Malhi Y, Nobre AD, Rastetter EB, Grace J, Pereira MGP (1998) Seasonal variation in net carbon exchange and evapotranspiration in a Brazilian rain forest: a modelling analysis. Plant, Cell & Environment, 21, 953-968. doi: 10.1046/j.1365-3040.1998.00339.x

Williams M, Rastetter EB, Fernandes DN, Goulden ML, Wofsy SC, Shaver GR, Melillo JM, Munger JW, Fan SM, Nadelhoffer KJ (1996) Modelling the soil-plant-atmosphere continuum in a Quercus–Acer stand at Harvard Forest: the regulation of stomatal conductance by light, nitrogen and soil/plant hydraulic properties. Plant, Cell & Environment, 19, 911-927. doi: 10.1111/j.1365-3040.1996.tb00456.x

Wright IJ, Reich PB, Cornelissen JHC, Falster DS, Groom PK, Hikosaka K, Lee W, Lusk CH, Niinemets Ü, Oleksyn J (2005) Modulation of leaf economic traits and trait relationships by climate. Global Ecology and Biogeography, 14, 411-421. doi: 10.1111/j.1466-822x.2005.00172.x

Wright IJ, Reich PB, Westoby M (2001) Strategy shifts in leaf physiology, structure and nutrient content between species of high-and low-rainfall and high-and low-nutrient habitats. Functional ecology, 15, 423-434. doi: 10.1046/j.0269-8463.2001.00542.x

Wright IJ, Reich PB, Westoby M, Ackerly DD, Baruch Z, Bongers F, Cavender-Bares J, Chapin T, Cornelissen JH, Diemer M, Flexas J, Garnier E, Groom PK, Gulias J, Hikosaka K, Lamont BB, Lee T, Lee W, Lusk C, Midgley JJ, Navas ML, Niinemets U, Oleksyn J, Osada N, Poorter H, Poot P, Prior L, Pyankov VI, Roumet C, Thomas SC, Tjoelker MG, Veneklaas EJ, Villar R (2004) The worldwide leaf economics spectrum. Nature, 428, 821-7. doi: 10.1038/nature02403

Wright IJ, Westoby M (2002) Leaves at low versus high rainfall: coordination of structure, lifespan and physiology. New Phytologist, 155, 403-416. doi: 10.1046/j.1469-8137.2002.00479.x

Wright JK, Williams M, Starr G, Mcgee J, Mitchell RJ (2013) Measured and modelled leaf and stand-scale productivity across a soil moisture gradient and a severe drought. Plant Cell and Environment, 36, 467-83. doi: 10.1111/j.1365-3040.2012.02590.x

Wu J, Albert LP, Lopes AP, Restrepo-Coupe N, Hayek M, Wiedemann KT, Guan K, Stark SC, Christoffersen B, Prohaska N, Tavares JV, Marostica S, Kobayashi H, Ferreira ML, Campos KS, Da Silva R, Brando PM, Dye DG, Huxman TE, Huete AR, Nelson BW, Saleska SR (2016) Leaf development and demography explain photosynthetic seasonality in Amazon evergreen forests. Science, 351, 972-6. doi: 10.1126/science.aad5068

Xu B, Park T, Yan K, Chen C, Zeng Y, Song W, Yin G, Li J, Liu Q, Knyazikhin Y (2018) Analysis of global lai/fpar products from viirs and modis sensors for spatio-temporal consistency and uncertainty from 2012–2016. Forests, 9, 73. doi: 10.3390/f9020073

Xu L, Baldocchi DD (2004) Seasonal variation in carbon dioxide exchange over a Mediterranean annual grassland in California. Agricultural and Forest Meteorology, 123, 79-96. doi: 10.1016/j.agrformet.2003.10.004

Xu X, Medvigy D, Joseph Wright S, Kitajima K, Wu J, Albert LP, Martins GA, Saleska SR, Pacala SW (2017) Variations of leaf longevity in tropical moist forests predicted by a trait-driven carbon optimality model. Ecology letters, 20, 1097-1106. doi: 10.1111/ele.12804

Xu X, Medvigy D, Powers JS, Becknell JM, Guan K (2016) Diversity in plant hydraulic traits explains seasonal and inter-annual variations of vegetation dynamics in seasonally dry tropical forests. New Phytologist, 212, 80-95. doi: 10.1111/nph.14009

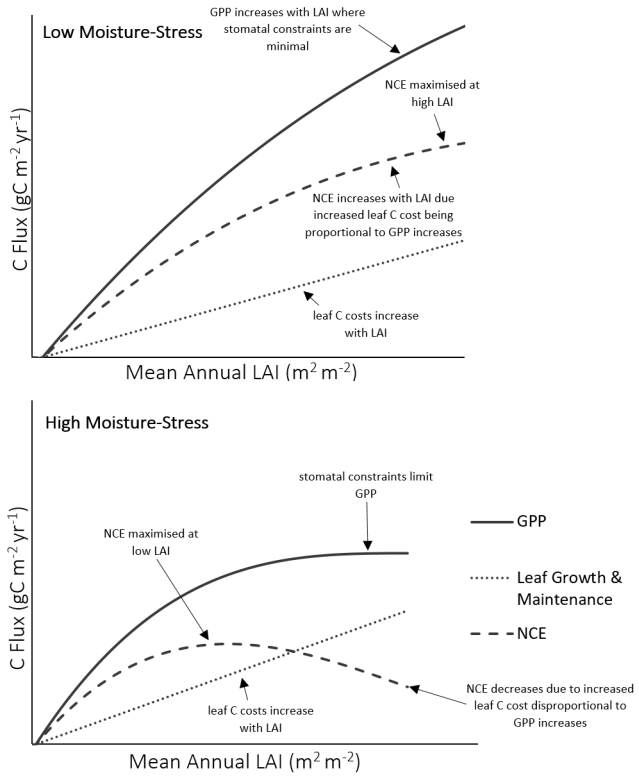

gcb_15368_f1.png

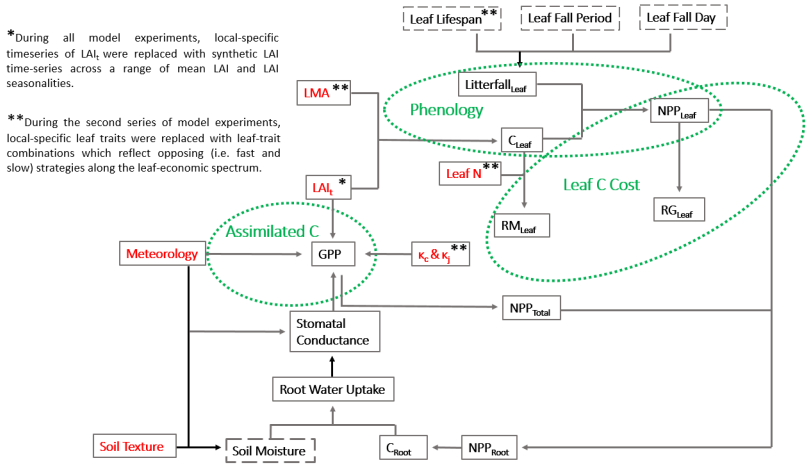

gcb_15368_f2.png

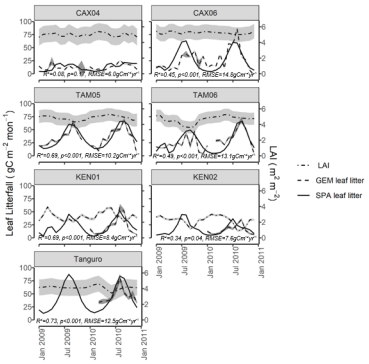

gcb_15368_f3.png

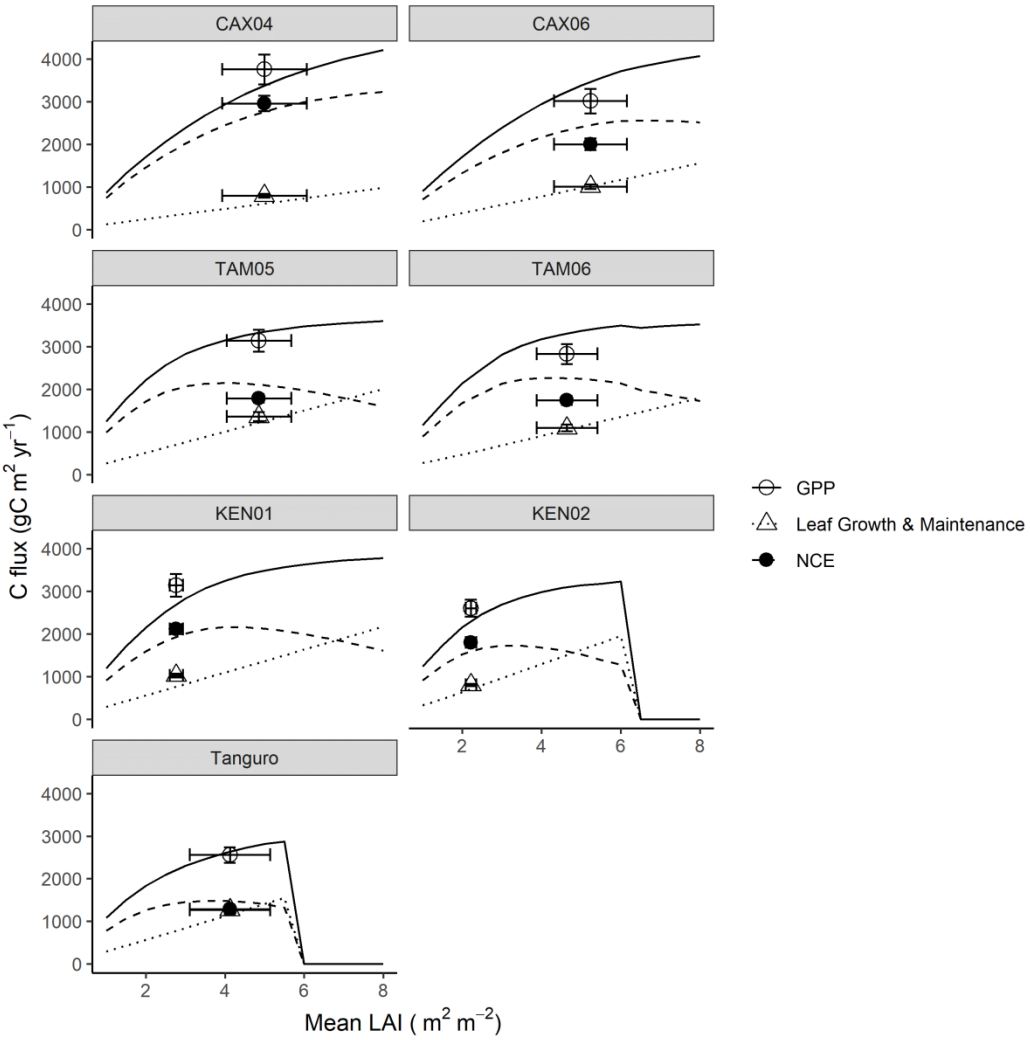

gcb_15368_f4.png

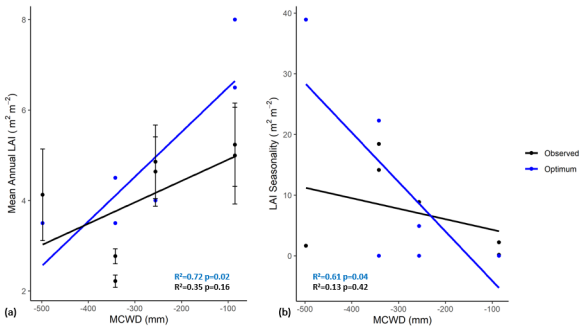

gcb_15368_f5.png

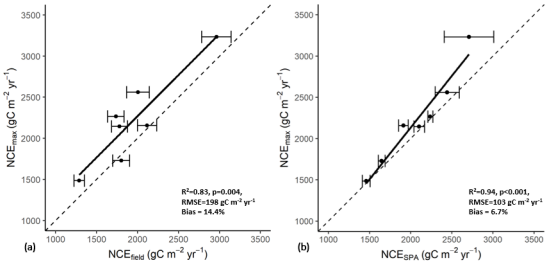

gcb_15368_f6.png

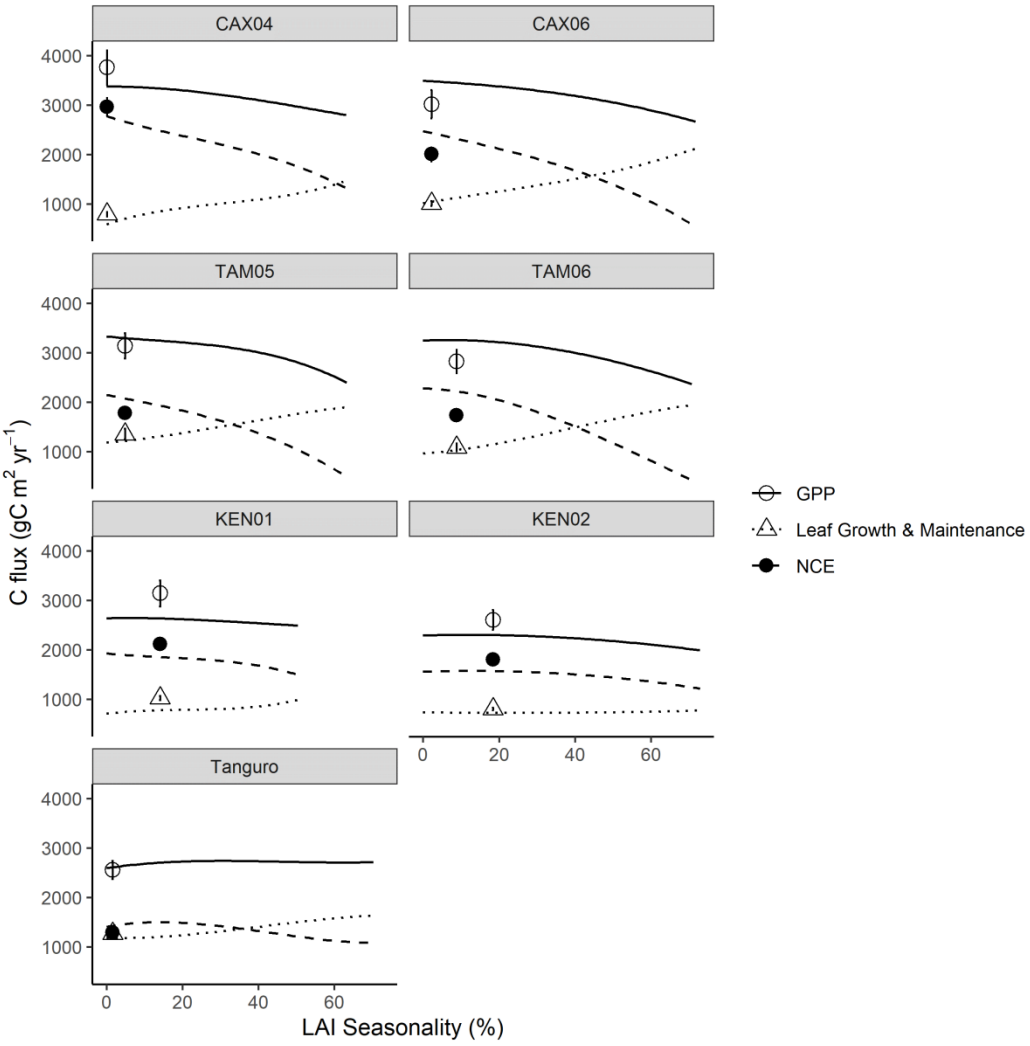

gcb_15368_f7.png

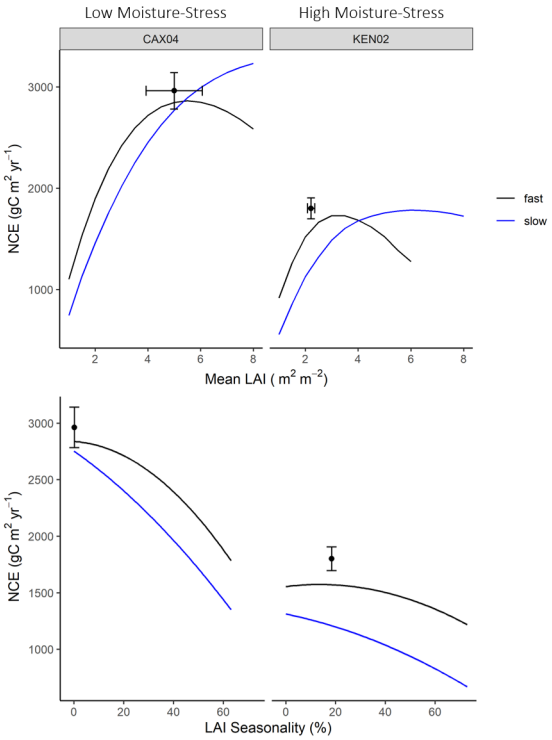

gcb_15368_f8.png